

LINZHI ZHANG

Integrated Stratigraphy and Fluvial Cyclicality of the Westphalian B in the southern North Sea Basin

Integrated Stratigraphy and Fluvial Cyclicality of the Westphalian B in the southern North Sea Basin

By

LINZHI ZHANG

Master of Science
in Geo-Energy Engineering

at the Delft University of Technology,
to be defended publicly on Monday, July 12, 2021, at 9:00 AM.

Supervisor:	dr. Hemmo A. Abels	
Thesis committee:	Prof. dr. Allard W. Martinius	TU Delft
	dr. Anne Pluymakers	TU Delft
	Timothy Baars, MSc	TU Delft

An electronic version of this thesis is available at <http://repository.tudelft.nl/>.

Contents

Abstract	5
Acknowledgments	7
1 Introduction	8
2 Geological Setting	12
2.1. Overview stratigraphy and formations	12
2.2. Structure	14
2.3. Westphalian B and lower Westphalian C	15
3 Dataset	20
4 Methodology	23
4.1. Electrofacies	24
4.2. Biostratigraphy	28
4.3. INPEFA stratigraphy	28
4.4. Lithostratigraphy	30
5 Results	32
5.1. Electrofacies	32
5.2. Biostratigraphy	37
5.3. INPEFA stratigraphy	39
5.3.1 Medium-term INPEFA of GR	39
5.3.2 Comparison between Biozones and INPEFA stratigraphic packages	42
5.3.3 Short-term INPEFA of POTA	44
5.4. Coal seams correlation	45
5.5. Correlation of cyclothem	47
6 Discussion	49
6.1. Limitation and reliability of the results	49
6.2. Integrated stratigraphy	51
6.3. Cyclothem and short-term INPEFA cycles	52
6.4. Astronomical forcing and climate-controlled cycles	53
7 Conclusion	57
Bibliography	59
Appendix A. Histogram of the percentage of different electrofacies in different stages	63
Appendix B. Thickness distribution of Biozones and INPEFA stratigraphic packages	64
Appendix C. 2D map of each identified biozone	65
Appendix D. 2D map of each INPEFA stratigraphic package	66
Appendix E. Long section of integrated stratigraphy	67

Abstract

The upper Carboniferous in the southern North Sea, especially the Westphalian B and lower Westphalian C stage is characterized by the deposited cyclothems that are a series of coarsening-upward fluvial sediments cycles. These cyclothems are often coal-bearing and no more than 15 m. Studying the fluvial cyclicity has a good potential for improved stratigraphy because the cyclothems show cyclic signals and provide a possible way of high-resolution correlation. An integrated approach using multiple approaches to come to a solid outcome also enables improving the stratigraphy. The previous studies mainly focused on large-scale stratigraphy with a vertical resolution of a few hundred meters. This study has analyzed the fluvial cyclicity and constructed an improved stratigraphic framework of Westphalian B and lower Westphalian C to better understand the sedimentary system. An integrated approach including lithostratigraphy, biostratigraphy and Integrated Predictive Error Filter Analysis (INPEFA) is applied to the series.

Six intermediate-scale biozones with a thickness of tens of meters to around 150 m are applied. Six intermediate-scale units named stratigraphic packages were recognized by INPEFA curves of the gamma-ray log. The correlations of the biozones and the stratigraphic packages are consistent with each other, and the offset between the boundaries of these two zonations is generally between 2-15 m. Individual intermediate-scale units have a highly variable thickness and the standard deviation of one unit can be up to 42 m. Constrained by the biozones and INPEFA stratigraphic packages, four main coal seams are correlated and their lateral extent can reach 15 km.

The small-scale cyclothems that range from 7 to 15 m can be extracted by INPEFA of potassium content log, referring to the small-scale INPEFA cyclicity. The cyclothems and the corresponding INPEFA cycles are thicker and better developed in the southern area. The average thickness of small-scale cycles is 12 m and these cycles are related to obliquity with a duration of approximately 35 kyr. The duration of Westphalian B calculated by the number and the time span of obliquity-scale cycles is nearly 1.2 Myr. No long-period, 100 & 400 kyr eccentricity cycles were recognized in this study.

Acknowledgments

I am thankful to the people contributing to the finalization of my thesis project since it is not easy to work on a Master's thesis project, especially in the special case of epidemic isolation. I would wish to express my deepest gratitude to my thesis supervisor Dr. Hemmo Abels and my daily supervisor Ph.D. candidate Timothy Baars for introducing me to this excellent and challenging topic and providing me with fruitful discussions, guidance, and suggestions. Secondly, I would like to thank Dr. Allard Martinius and Dr. Anne Pluymakers for being part of my graduate committee and offering much useful input for my thesis project. Besides, Richard Huis in 't Veld, who has worked on the North Sea basin for a long time, is thanked for the provided biozones and discussion during the work. Last but not least, I would like to thank my parents, family members, and friends for their moral support and Wintershall Noordzee for providing the dataset. This work has been performed within the frame of the TopSectors FRESCO project at TU Delft.

1 Introduction

High-resolution stratigraphy of 3D sedimentation through time is needed for subsurface engineering applications since the stratigraphic framework can lead to a better prediction of the reservoir quality and optimal strategies for production. However, it is difficult to accurately develop a high-resolution stratigraphy with limited data since the controlling factor of a sedimentary system is often controversial. Generally, the sedimentary units are controlled by both allogenic and autogenic processes. Allogenic processes, usually caused by climate, tectonics, and sediment input, are thought to be able to occur on a basin or even global scale (Cecil, 2003). In contrast, autogenic processes are local because they are introduced by the sedimentary system itself. It is hard to completely untangle the effects of different types of processes in the previous sedimentary system located underground.

The upper Carboniferous is known for its characteristic fluvial cyclic patterns called cyclothems (Weller, 1930) consisting of coal-bearing deposits and is widely assumed to be related to glacio-eustatic sea level, tectonic subsidence, and sedimentation (Wilkinson et al., 2003; Weedon and Read, 1995). Studying the fluvial cyclicity has a good potential for improved stratigraphy because the cyclothems show cyclic signals and provide a possible way of high-resolution correlation (Henderson et al., 2020). The cyclic signals refer to the cyclic sedimentation that changes repeatedly in the depositional systems. The cyclic sediments comprise different types of rock and show repeating patterns (Ferrero and Celestina, 2004). An integrated approach using different stratigraphic methods to come to a solid outcome can also improve the stratigraphy. The integrated stratigraphy often contains lithostratigraphy, biostratigraphy, isotope stratigraphy, and cyclostratigraphy.

The upper Carboniferous has been studied in different areas for the past decades. For instance, eccentricity cycles (~100 kyr) in Ostrava formation, Upper Silesian Basin located in the Czech Republic were defined (Jirasek et al, 2018). Two conceptual models for peat formation in a lower Palaeocene fluvial system, north-eastern Montana in the USA was generated (Noorbergen et al, 2018). Astronomical cyclicity in Upper Carboniferous fluvial-deltaic sediments in the subsurface of the Netherlands was studied by Bosch (2008) and a high-resolution stratigraphic correlation of Rotliegend deposits in the central Dutch offshore has been made (De Jong et al, 2020).

The upper Carboniferous in the southern North Sea (Fig. 1.1) does not contain detailed, high-resolution correlations. The previous studies mainly focused on the regional, large-scale stratigraphy related to the third order in sequence stratigraphy. The vertical resolution often ranges from nearly 150 meters to several hundred meters. Some intermediate-scale stratigraphic frameworks with a vertical resolution of more than 50 meters to around 150 meters are available. But these stratigraphic correlations utilized a single approach

like the biostratigraphic method, the lithostratigraphic method, and these stratigraphic frameworks are independent of each other. Specifically, O'Mara has classified detailed facies and interpreted sequence stratigraphy in third-order (O'Mara, 1995; O'Mara and Turner, 1997; O'Mara and Turner 1999). Several marine bands which are commonly dark-colored shale rich in marine fossils play important roles in the determination of stratigraphic zonation. McLean (1996, 2005) synthesized biozonation based on miospore taxa and a limited number of macrofaunal control points. De Jong et al. (2007, 2020) used the climate stratigraphic method to make a subsurface correlation in the Upper Carboniferous of Anglo-Dutch basin and central Dutch offshore. Therefore, an improved integrated stratigraphy with a vertical resolution of tens of meters or even a vertical scale of 10 to 20 meters is expected and the cyclicity analyses are of great importance.

Regional (sub) stages (Western Europe)		Lithostratigraphic schemes UK (north) - Cameron 1993b		Lithostratigraphy UK - Besly 2002	Lithostratigraphy UK - Camonron 2005	Lithostratigraphy - Wintershall/ In this study	
Asturian	Westphalian	D	Schooner Formation	Upper Ketch Unit	Boulton formation	Ketch member	Boulton formation
				Lower Ketch Unit	Upper Ketch member		Upper Ketch member
Bolsovian		C	Lower Schooner Unit	Lower Ketch member	Lower Schooner unit	Lower Schooner unit	Lower Ketch member
				Upper Cleaver member			Upper Cleaver member
Duckmantian	B	Westoe Coal Formation	Lower Cleaver member	Westoe Coal Formation	Westoe Coal Formation	Lower Cleaver member	
			Westoe formation			Upper Westoe Coal formation	
						Lower Westoe Coal formation	
Langsettian	A	Caister Coal Formation	Caister Coal Formation	Caister Coal Formation	Caister Coal Formation	Caister Coal Formation	
					Caister Sanstone unit	Caister Sanstone unit	

Fig.1.1 Summary of substages and lithostratigraphy of Westphalian stage for the northern UK and western Europe. Different names were given to the same substages or lithostratigraphic units. No vertical scale implied.

In order to study the fluvial cyclicity and develop an improved stratigraphy in the upper Carboniferous of the southern North Sea basin, the Westphalian B and lower Westphalian C being a part of the upper Carboniferous deposits (Fig. 1.1) are the best targets. The Quadrant 44 and a small part of Quadrant 49, as well as part of nearby Dutch D and E quadrants, are good to start (Fig. 1.2). The area of interest has a long

history of gas production resulting in high data availability including wireline well logs and cores. The dominant sediments deposited in the interval are alluvial and upper delta plain associations consisting of abundant coal seams as well as fluvial-deltaic sandstones, siltstones, and shales (O'Mara, 1995; Kombrink, 2008). Different types of rock, especially coal seams and marine bands repeatedly occur (O'Mara and Turner 1999) and the astronomical cyclicity of Westphalian B and C in the onshore of the Netherlands which is near the study area has been studied (Bosch, 2008; De Jong et al., 2020). Furthermore, the later Westphalian formations including upper C and D were severely eroded by Base Permian Unconformity (BPU) while the preservation of Westphalian B and lower Westphalian C are relatively good and shown in many wells in Quadrant 44 and 49 (Cameron et al, 1997; Schrijver et al, 2020).

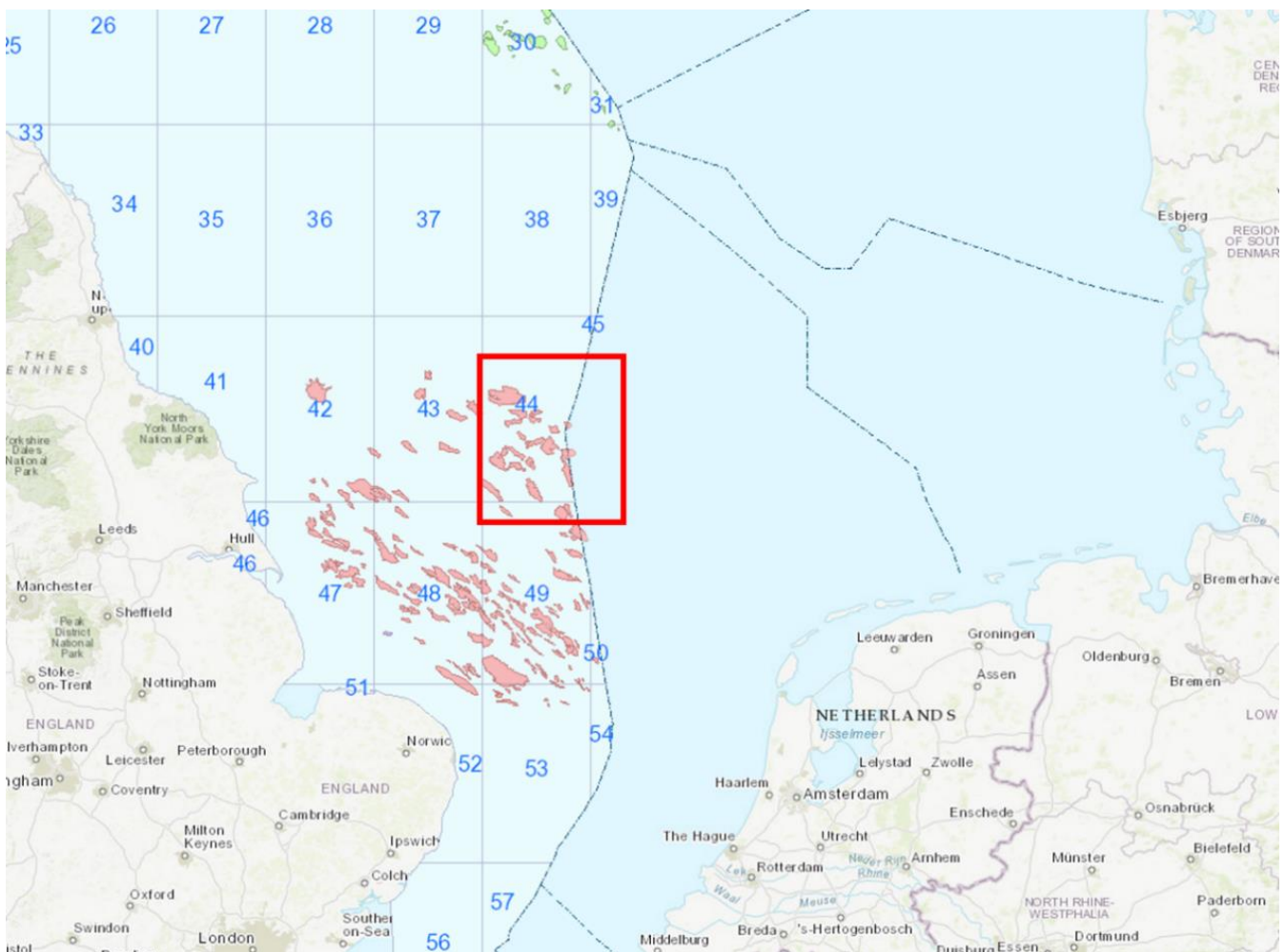


Fig. 1.2 The map showing the study area consisting of Quadrant 44, part of Quadrant 49, part of Dutch Quadrant D, and Dutch Quadrant E (marked in red square). The red polygons represent oil and gas fields. This map is taken from Oil & Gas Authority, UK.

Therefore, an integrated stratigraphy for the Westphalian B and lower Westphalian C in the study area is expected to establish. To achieve the goal, the research questions of this study are:

- What is the character of sedimentary cyclicity in the Upper Carboniferous successions?
 - What is or are the vertical scale or scales?

- What is the lateral consistency and heterogeneity of the cyclicity?
- Can the identified cyclicity be related to astronomical climate forcing?
- Can an improved integrated stratigraphy produce more reliable correlations at the 10s-of-meters scale?

The orbital forcing and allogenic signals that are essential to cyclicity study are hard to directly detect, especially in the subsurface. And they are often interacting with other factors controlling sedimentation. Thus, the recognition and analyses of the fluvial cyclicity need assistance from the integrated stratigraphic approach and previous studies. The integrated approach in this study includes biostratigraphy, lithostratigraphy, and Integrated Predictive Error Filter Analysis (INPEFA). Biostratigraphy was developed in view of palynology applied to cuttings or some core materials (McLean, 1996; McLean 2005), and some wells in this area have reported detailed palynology. Although biostratigraphy has some limitations and measurement can have errors of the order of meters, its framework still provides important clues for an intermediate-scale stratigraphical correlation. INPEFA is thought to be related to climate change and astronomical forcing (Nio et al., 2005; De Jong et al., 2020). The application of INPEFA in the upper Carboniferous of onshore and offshore Netherlands can also be a strong tool to aid in understanding the fluvial cyclicity and constructing a stratigraphic framework. Additionally, lithostratigraphy will also be involved since the lithofacies in the different parts of the formations show various characteristics (O'Mara and Turner, 1999). Among them, the indications of thick coal seams and marine bands could be useful because they can be widely distributed. However, marine bands are hard to be distinguished in the subsurface due to the different petrophysical responses (O'Mara, 1995).

In this thesis, the geological setting of the study area will be introduced at the beginning to give a first view of the sedimentary system. Then, the integrated approach including biostratigraphy, INPEFA stratigraphy, and lithostratigraphy will be explained and applied to several wells in the study area. Considering the manual identification of lithofacies is time-consuming and subjective, automatic interpretation of sedimentary facies will be developed before the integrated stratigraphic method. Afterward, the results of a single method and the comparison of different methods will be provided in order to study the potential cyclicity and develop improved stratigraphy. By the end of this study, a discussion about the reliability of the results and the astronomical forces will be presented.

2 Geological Setting

2.1. Overview stratigraphy and formations

The upper Carboniferous period in the southern North Sea dominantly consists of the Westphalian stage deposits aged 300 Ma. The sediments deposited in the same stage have various names in different areas (Fig. 1.1). The Westphalian can be subdivided into Westphalian A, B, C, and D from bottom to top, containing four different sedimentary associations, but the stratum in the upper Westphalian C and Westphalian D in the southern North Sea are often invisible due to the severe erosion caused by BPU (Cameron et al, 1997; Schrijver et al, 2020).

Three formations with various lithofacies and sedimentary patterns were defined in the Westphalian B and lower Westphalian C, from bottom to top namely Caister sandstone formation, Westoe Coal formation, and Cleaver formation (Fig. 1.1, Fig. 2.1). The boundaries of the formations developed based on lithofacies vary in different studies and they are accepted to be regionally diachronous (Cameron, 1993b; Besly, 2002; Cameron et al, 2005). The Caister sandstone formation is also known as Murdoch sandstone. Westoe Coal formation can be divided into two parts according to the frequency of coal seams and different biological areas, which will be explained in part 2.3. Also, the Cleaver formation was considered to be subdivided into upper and lower parts.

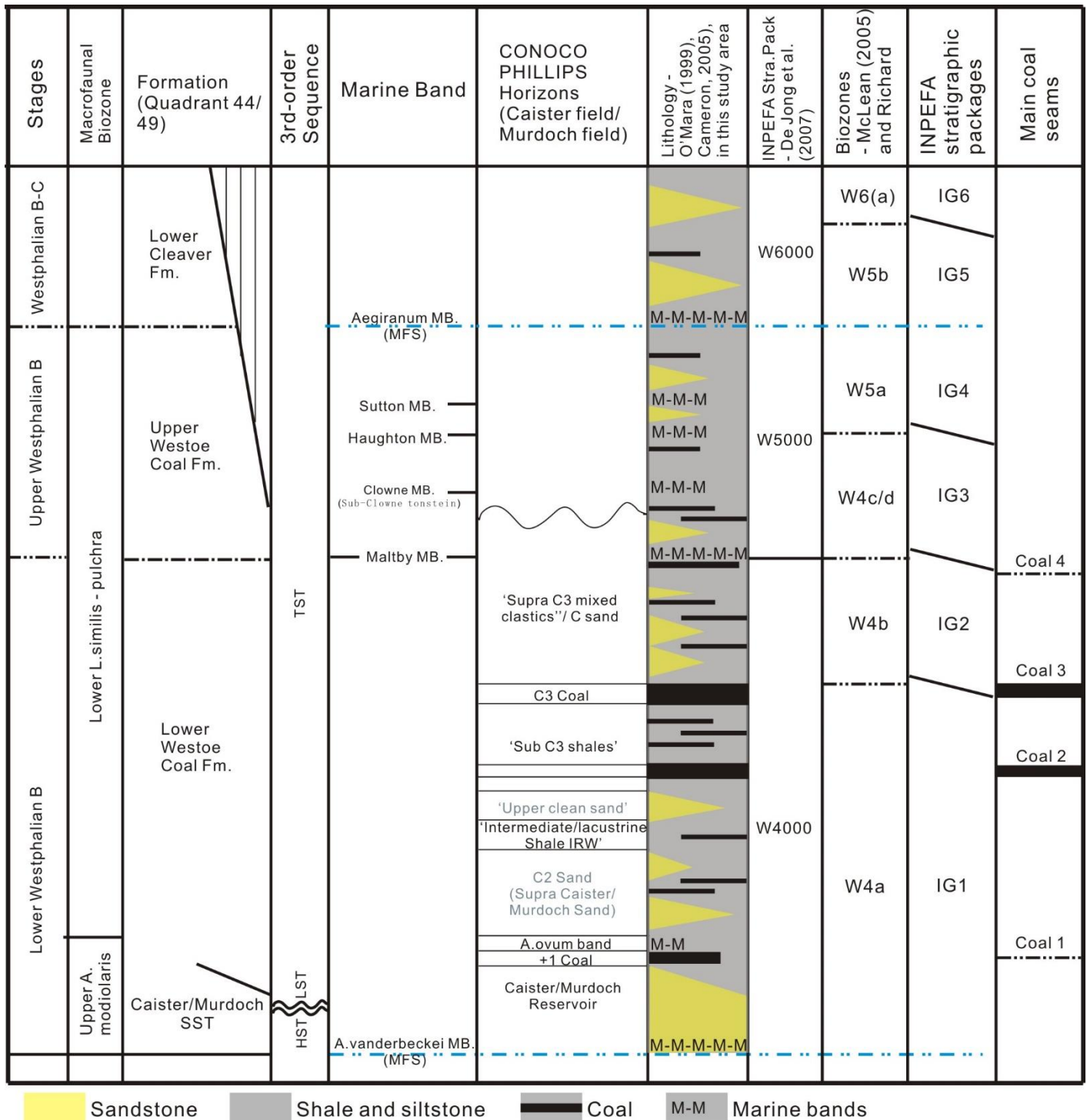


Fig. 2.1 Overall stratigraphy of Westphalian B and lower Westphalian C stage for the study area. The figure contains biostratigraphy, lithostratigraphy, sequence stratigraphy, marine bands, and INPEFA stratigraphy. The dashed lines indicate the boundaries are not solid surfaces. The last three columns are the results of this study, which will be explained in the following parts. No vertical scale implied.

2.2. Structure

The southern North Sea basin is located on the east of the United Kingdom continental shelf and close to the Netherlands, covering an area of 36,951 km². It underwent multiple stages of evolution in geological history. From the middle Carboniferous up to Westphalian C, tectonics went through uniform thermal subsidence (McKenzie D, 1978; Schroot B M et al, 2003; Bailey J B et al, 1993). Due to the reactivation of base faults during the post-rifting stage, an NW-SE-trending graben system around the basin was formed from late Carboniferous to early Permian. As a result, the Carboniferous formations were folded and, especially Westphalian C and D were eroded in Permian time creating the BPU (Stewart and Coward, 1995; Schroot B M et al, 2003). The deposits of Westphalian in the filling basin were widely thought to be a northerly source (Schroot B M et al, 2003). However, based on the heavy-mineral data, more than one provenance could exist. Collison (2005) thought the source of Cleaver formation could lay to the south, while the sediments for the Westoe Coal formation may be shed from the Wales-Brabant High, and the southward source from Variscan terrain cannot be ruled out.

The southern North Sea covers an area from the central Quadrant of 42 to 44 and southern parts of 48 and 49 quadrants. The study area, Quadrant 44 and the north part of Quadrant 49 (Fig. 2.2), is situated in the inner Silver Pit Basin. Some NW-SE trending faults and folds had been developed inside Silver Pit Basin. The nearby Quadrant E and D in the Dutch sector is on the Cleaver Bank High which is a high platform comprising multiple deformations resulting from both folding and faulting (Schroot B M et al, 2003).

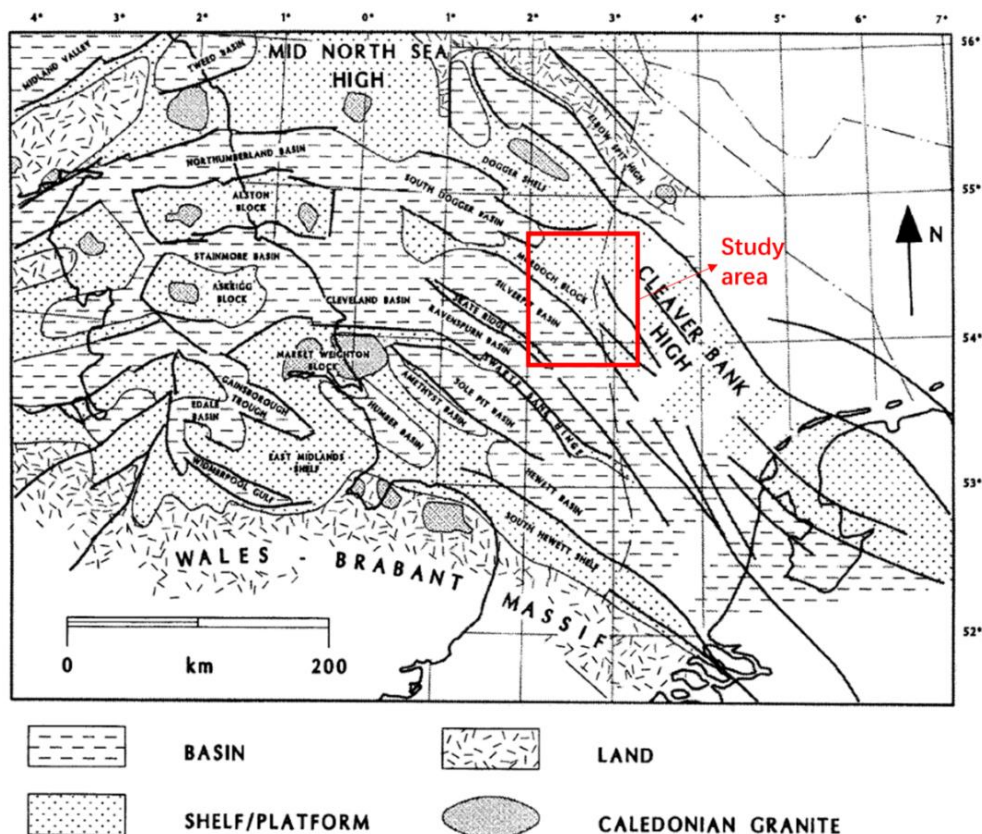


Fig. 2.2 Structural framework during Early Carboniferous showing the paleotopography (from Besly, 1998). Note that the study area covers Quadrant 44 and part of Quadrant 49 in the offshore UK, and a small part of Quadrant D, E in the offshore Netherlands.

2.3. Westphalian B and lower Westphalian C

Westphalian deposits are well known as coal-bearing rocks, especially in the Westphalian B stage. The main sedimentary facies present are Lower Delta Plain, Alluvial, and Upper Delta Plain Associations corresponding to Westphalian A/B/C, respectively (O'Mara, 1995; Kombrink, 2008). In Westphalian B and C, the fluvial-deltaic sediments were deposited in low relief, humid environments. The coastal alluvial plain is dominant, consisting of crevasse splay and minor distributary channel deposits prograding into lacustrine and floodplain fills (O'Mara, 1995; O'Mara and Turner, 1999). The sandstone content was thought to decrease southward as a result of south-southwest trending palaeoslope where channel system from northern source passed through (Besly, 1990; Collinson et al, 1993; O'Mara, 1995).

The Westphalian B and lower Westphalian C sediments are believed to be primarily deposited during a Transgressive Systems Tract (TST) while the lower sand-bodies were thought to be deposited during a Highstand Systems Tract (HST) to Lowstand Systems Tract (LST) (O'Mara, 1995; Quirk, 1997; Schrijver et al, 2020).

The lower and upper boundaries of Westphalian B are two, third-order marine bands (MB), namely Vanderbeckei MB and Aegiranum MB, respectively (O'Mara, 1995; Quirk, 1997). When the transgressive sequence set formed, it was frequently influenced by marine incursion. Several fourth-order marine bands developed inside and the remarkable marine bands are Malby MB, Clown MB, Haughton MB, and Sutton MB. The Malby MB is considered the boundary between the upper and lower Westoe Coal formation (O'Mara, 1995; O'Mara and Turner, 1999; Schrijver et al, 2020). Marine bands reflect the fluctuation of sea level and subsequently, show the change of base level. They are commonly dark-colored shales, usually rich in marine fauna and organic materials and no more than 2 m (O'Mara, 1995). Marine bands often show uranium enrichment due to the anoxia conditions and low sedimentation rates (Fisher and Wignall, 2001). However, the wireline response characteristics, especially the uranium response of MBs in Westphalian B vary markedly (O'Mara, 1995). This raises the difficulty of recognition of MB in the subsurface without specific calibration of log response.

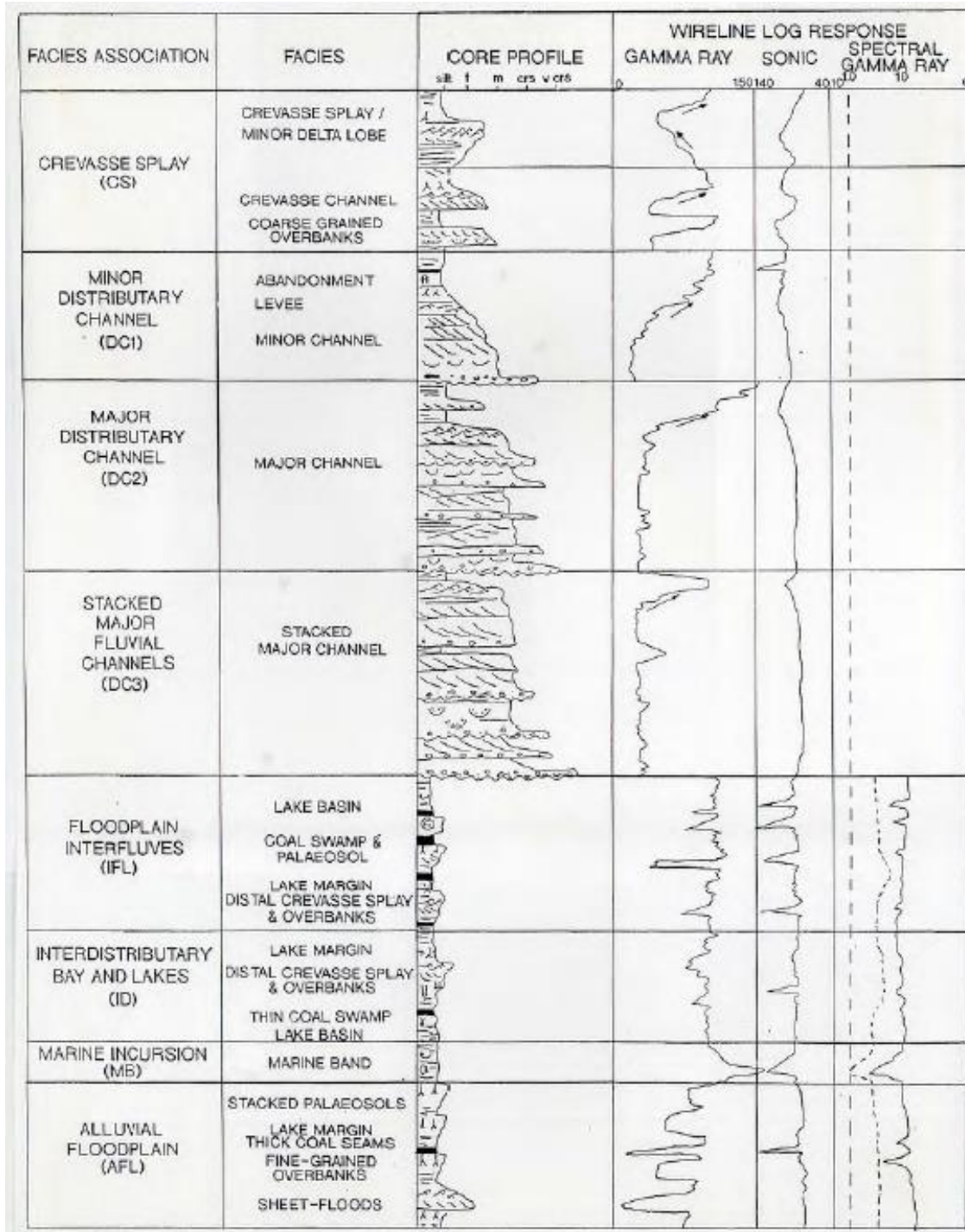


Fig. 2.3 Summary of sedimentary facies and wireline log facies in Westphalian B (from O'Mara, 1995)

The lower part of Westphalian B in the study area is Caister Sandstone deposited by low-sinuosity braided channels (O'Mara and Turner 1995, 1999). It is characterized by coarse, major-stacked sand-bodies, usually ranging from 30 to 40 m thick and covering an area over 250 km² (Ritchie and Pratsides, 1993; O'Mara, 1995). From bottom to top, the fluvial channel style gradually transformed to single and high-sinuosity, and thus, sandstones were interspersed in the Westoe Coal formation (O'Mara and Turner, 1999). With the development of the lake and floodplain, shale and coal seams frequently appear and were concurrent with the change of channel features. In the lower Westoe Coal formation, the coals are thicker

(≥3m) and more frequent compared with thinner and infrequent coals deposited in the upper Westoe Coal formation, which suggests a higher rate of stratigraphic base-level rise (Flint et al, 1995; O'Mara and Turner, 1999). Coal seams correlation combined with biostratigraphy has been worked in several studies because the wireline log response of coals is distinguishing and the coal seams are able to cover a large area within the low-relief area (Quirk, 1993; O'Mara and Turner, 1999).

Besides marine bands and coal seams, detailed sedimentary facies and electrofacies (Fig. 2.3) of upper delta plain and alluvial plain associations have been synthesized by O'Mara (1995) from a view of literature. The essential facies involve the distributary channel, interfluvial floodplain, interdistributary lake, stacked channel sands. They act as a good base for automatically interpreting electrofacies in this study. Stone et al (2010) also depicted an idealized schematic model within the upper delta plain depositional environment of the Westphalian, Pennine Coal Measures Group which is the same formation as the interval studied in this study but in the onshore area (Fig. 2.4). It enables to illustrate the lateral facies distribution, and both vertically and laterally reflect the relationship among different facies.

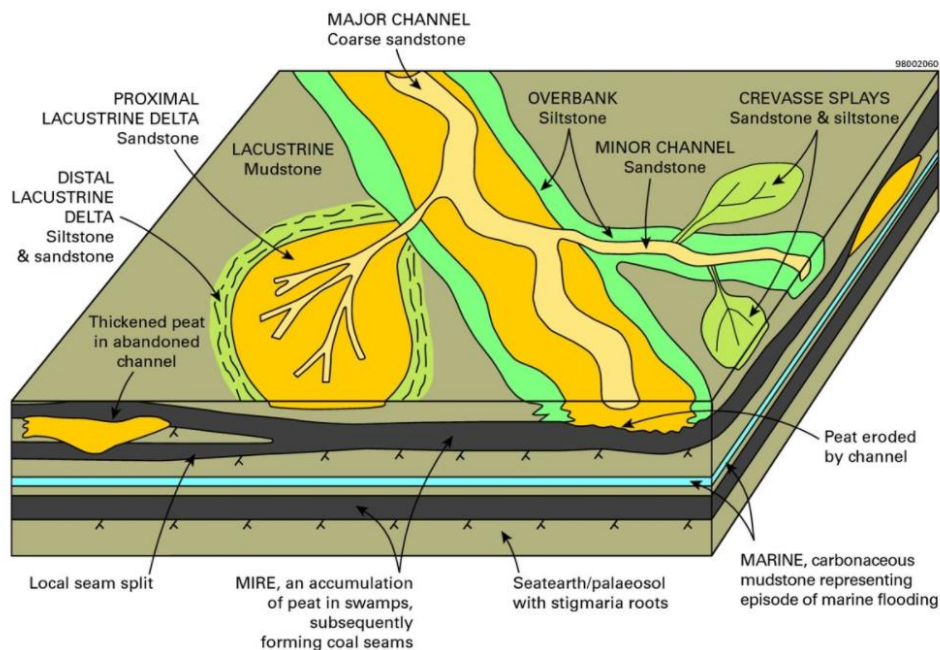


Fig. 2.4 Schematic illustration of the facies variation within the upper delta plain depositional environment of the Westphalian, Pennine Coal Measures Group (from Stone et al, 2010)

The repeating and coarsening-upward cyclic series which are also named cyclothems were deposited in the Westphalian B. They are usually capped by minor distributary channel sandstone or coals (O'Mara, 1995). Tucker et al (2003) generated an ideal scheme of this type of cyclothems deposited in the transgressive system (Fig. 2.5). The sequence of deposition they follow is mudstone at the bottom, then sandstone overlying siltstone, and finally palaeosol and coal seams (Tucker et al, 2003). Sometimes the upper coal seams might be oxidized after depositing or might not form, which depends on the sedimentary environment. The ideal cyclothems were thought to be formed when a channel moved into a lake at the

beginning. Then it was abandoned, overlaid by vegetation and swamp to deposit seatearths and coals (Tucker et al, 2003). In other words, the formation of each cyclothem is related to a flooding event. The thickness of coal-bearing cyclothem developed in the study area is commonly no more than 15 meters. The vertical scale of the cyclothem is defined as a small scale in this study, referring to the short term in cyclostratigraphy, and fifth order in sequence stratigraphy.

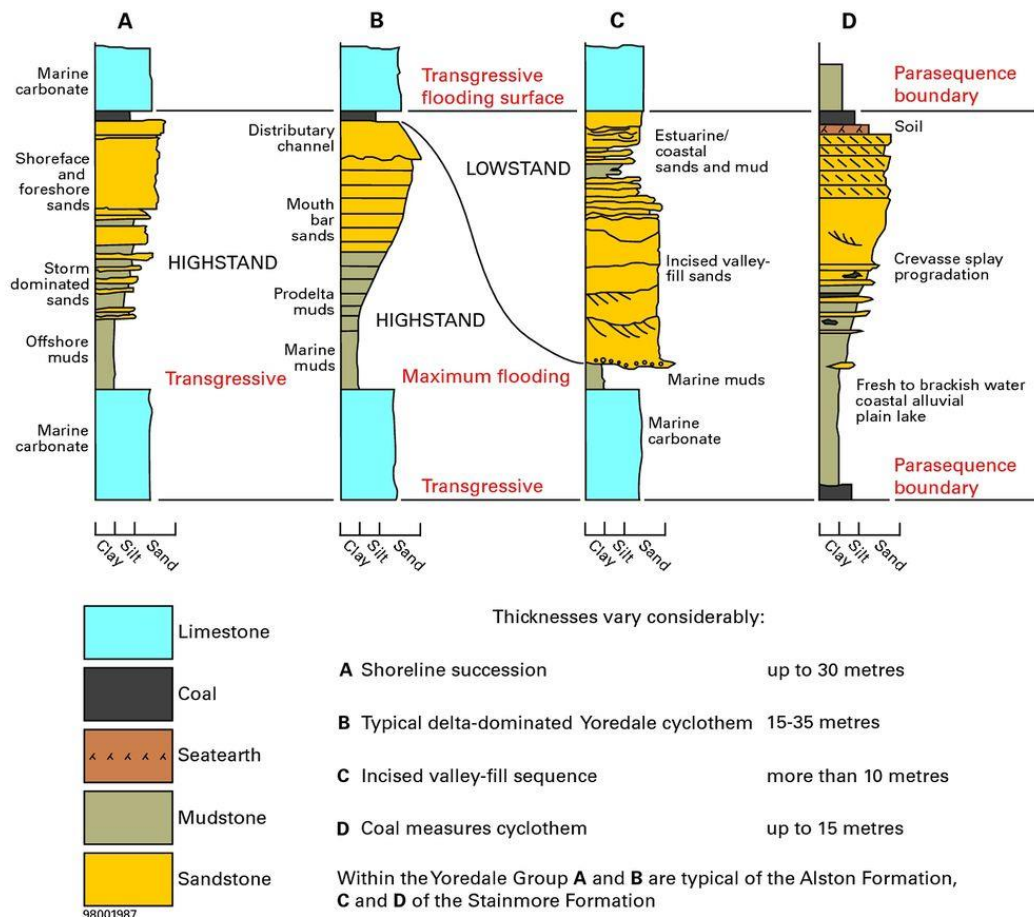


Fig. 2.5 Illustrative logs and interpretations for some types of high-frequency clastic sequences within the Yoredale and Pennine Coal Measures groups of northern England (from Tucker et al, 2003)

In the previous study, the identification of marine bands and the correlation of coal seams are strongly related to palynology. Hence, miospore biostratigraphy has been studied for a long time and the classified biozones are widely accepted. The offshore biozones in the North Sea are defined on the last occurrence of specific taxa which consistently show in the interval of drilling cuttings and core materials (Ritchie and Pratsides, 1993; McLean, 2005). The recent palynostratigraphy in Westphalian B (Fig. 2.6) contains W4 and part of W5 biozones, inside which four sub-biozones were divided. From bottom to top they are W4a/W4b/W4c/W5a (McLean, 2005). Since the interval of interest in this study contains part of Westphalian C, another two biozones which are W5b and W6 are included. The Duckmantian stage corresponds to Westphalian B and the Bolsovian stage represents Westphalian C (Fig. 2.6). According to the updated

correlation of biozones for several wells in Quadrant 44 and 49 from Wintershall Noordzee (personal communication), not all wells with Westoe Coal formation and Cleaver formation have complete biozones of Westphalian B from W4a to W5a. Although the thickness of biozones greatly varies, it is usually between tens of meters and nearly 150 meters. In this study, the vertical scale of the detailed biozones is defined as an intermediate scale.

Stages	Palynostratigraphy				
	Biozones	Sub-Biozones	Defining criteria	Associated range tops	Associated range bases
Westphalian D (pars.)	W7	W7c	S. dimorphus	[V. laevigata, E. zonalis, S. radiatus, A. hoffmeisterii, Zonalosporites spp.] - C. kosankei acme	▲ - S. camptotus
		W7b			
		W7a	V. cancellata	[C. solaris, V. magna, A. triquetrus, R. falsus, R. speciosa, T. tribullatus]	▲ - S. dimorphus, C. annulatus, L. gigantea, ▲ - T. verrucosa, T. obscura
Bolsvian	W6	W6b	D. bireticulatus	- C. lorricatus	▲ - T. pseudothiessenii
		W6a	A. spinososaetosus	[D. gracilis, R. faunus, R. tenuis, R. fulva, V. microverrucosus] - R. medietreticulatus, A. pustulatus, V. tortuosa, S. mux, R. reticulocingulum, R. polygonalis	▲ [R. aculeata, B. haaksbergensis, K. glomus, L. trileta] ▲ - Z. magnus, Punctatosporites spp. acme
	W5	W5b	G. varioreticulatus	- G. papillosus, R. fulva acme	▲ - P. obliquus, T. securis, V. fenestrata
		W5a	C. connexus	- L. rotunda, R. cf. striatus	
Duckmantian	W4	W4c	T. sculptilis	[D. duriti, A. multiplicatus, A. guerickei, T. triquetrus, D. swadei, M. intorta, P. fragila, C. bucculentus, L. rotunda acme]	▲ - P. rotundus, T. sculptilis acme, V. magna acme
		W4b	L. noctuina noctuina acme	[S. concavus, D. smithii, R. microhorrida, C. corrugatus]	▲ - T. sculptilis, V. magna, C. rigidus, P. granifer
	W4a	S. sinuatus	- L. nitida, L. noctuina noctuina	▲ - C. solaris	
	W3	W3a	S. rara	- P. mimutus, L. noctuina noctuina acme	
Langsettian	W2	W2b	R. aligerens	[S. pretiosus windsorensis, D. cf. spinosus, A. guerickei acme]	▲ - M. nobilis
		W2a	R. aligerens acme	[H. murchisonensis, R. striatus, A. echinatoides, T. diamphidites, D. karadenizensis, A. variocornuus]	▲ [M. harrisonii, R. faunus, R. tenuis, E. globiformis acme]
	W1	W1b	V. cancellata s.s.	- T. cf. protensus, C. splendidus, K. ornatus, D. probireticulatus, C. laminosa, W. polita	▲ [P. fragila, E. globiformis, V. donarii, V. pseudoreticulata]
		W1a	St. triangulus	- S. arenaceus	▲ [E. zonalis, F. pallidus, F. junior, V. cancellata, A. pustulatus s.s., R. cf. difformis]
	Yeadonian (pars.)	N5 (pars.)	N5c	A. nudus	[L. densus, A. pilus, C. bialatus, S. triangulus, P. ruginosus, S. triangularis] - T. nodosus, M. punctatus

Fig. 2.6 North Sea Westphalian biozones (from McLean et al, 2005). No vertical scale implied.

3 Dataset

Accurate and high-resolution stratigraphic correlation requires a large amount of data and different methods. Core materials are the most direct data, allowing access to the rocks and doing measurements such as fossil content or chemical composition. Wireline logs serving as second-hand data are objective and continuous, which can vertically extend to whole intervals. Besides, digital data can be processed and applied to mathematic methods to better understand and analyze.

Within the area of interest in this study, there are many gas fields with high well density. Most of the wells contain wireline log data and lithostratigraphy which was accepted by the Wintershall company. Some of the wells have bio-reports, core materials as well as man-made interpretations of lithofacies. Different types of logs are provided and the most useful data for this thesis are acoustic logging and nuclear logging data (Table. 3.1). The bio-reports and core photos of some wells are available on Oil & Gas Authority, British Geological Survey, and NLog Dutch Oil and Gas portal website. After looking through all available wells, not all wells have full Westoe Coal formation or Cleaver formation. For some wells, the Cleaver formation was eroded by overlaid BPU.

Table. 3.1 The conventional logging data provided in this project and their use in this thesis

Petrophysical logging data	Gamma Ray	Potassium	Uranium	Thorium	Caliper	Neutron Porosity	Bulk Density	Sonic
Abbreviation	GR	POTA	URAN	THOR	CALI	NPHI	DEN	DT
Usage in this thesis	√	√	√	√	×	×	√	√

There are 16 wells in the study area with detailed bio-reports and 15 wells covering both Cleaver formation and Westoe Coal formation. Besides, 6 wells have photos of borehole cores located in the interval of interest. Another well situated in onshore Netherlands namely KPK-01 will also be used. Its astronomical cyclicity in Westphalian B&C fluvial-deltaic sediments has been studied and suggested by Bosch's master thesis, which provides a good example to compare whether the results in this study show the same idea on astronomical forcing. Therefore, a total of 27 wells will be studied (Table. 3.2). The distance between most wells is relatively long, usually between several kilometers to ten kilometers (Fig. 3.1).

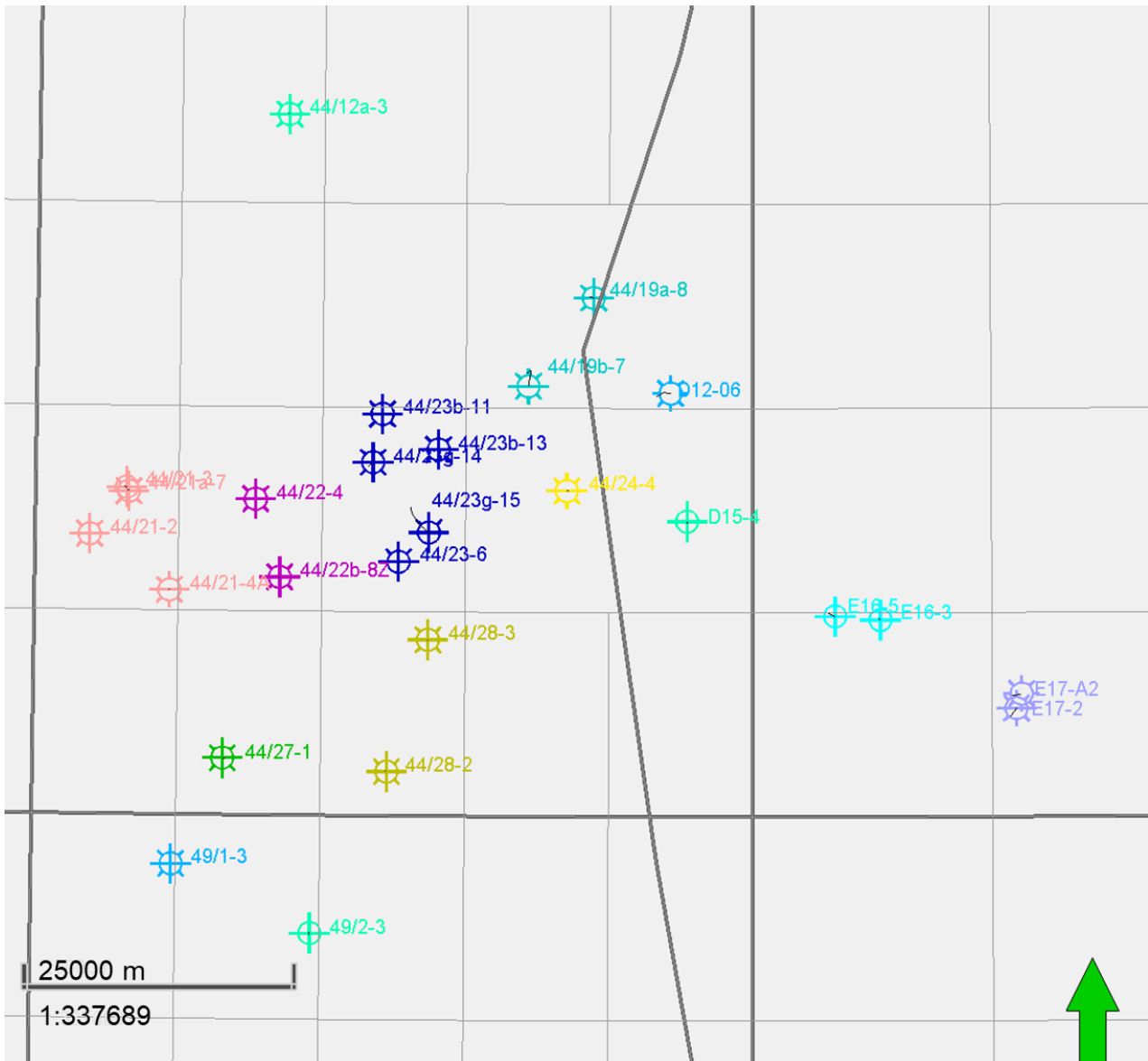


Fig. 3.1 The map shows the location of used wells (except KPK-01) in the study area. Most areas are in Quadrant 44. 2 wells in the south are situated in Quadrant 49. Part of Quadrant D and E in the offshore Netherlands are also involved.

Table. 3.2 Information of well conditions. If the log data of a well comprises GR, POTA, DEN, and DT log, √ was placed in the corresponding basket. If the formations of one well contain complete Cleaver formation and Westoe Coal formation, √ was given as well. The total thickness of the interval covers both Cleaver formation and Westoe Coal formation.

Wells	Biozones	Log data	Formation	Total thickness of interval (TVD) / m	Core materials
44/12a-3	W4a W4b	√	√	164.96	-
44/19a-8	W4a W4b W4c W5a	√	√	233.13	-
44/19b-7	W4a W4b W4c W5a	No URAN/POTA	√	197.83	-
44/21-2	-	√	√	432.13	√
44/21-3	W4a W4b W4c W5a W5b	URAN/POTA/DEN x complete	No Caister SST	-	-
44/21-4A	W4a W4b W4c W5a W5b	No URAN/POTA/DEN/DT	No Caister SST	-	-
44/21a-7	-	√	√	436.28	-
44/22-4	-	No URAN/POTA	No base Ketch	-	√
44/22b-8Z	W4a W4b W4c W5a W5b	√	No base Ketch	-	-
44/23-6	-	No URAN/POTA	No base Ketch	-	√
44/23b-11	W4a W4b W4c W5a W5b	√	No Caister SST	-	-
44/23b-13	W4a W4b W4c	√	√	277.84	-
44/23g-14	W4a W4b W4c W5a	No URAN/POTA	√	280.07	-
44/23g-15	W4a W4b W4c W5a	No URAN/POTA	√	297.28	-
44/24-4	W4a W4b W4c W5a	√	√	250.8	-
44/27-1	W4a W4b W4c W5a W5b W6a	URAN/POTA x complete	√	633.23	√
44/28-2	W4a W4b W4c W5a W5b W6a	√	√	542.92	√
44/28-3	-	√	No base Ketch	-	√
49/1-3	-	√	No Caister SST	-	-
49/2-3	W4a W4b W4c W5a W5b W6a	√	√	712.32	-
D12-06	W4a W4b W4c W5a	No URAN/POTA/DT	No Caister SST	-	-
D15-4	W4a W4b W4c	No URAN/POTA	No base Caister SST	-	-
E16-3	-	√	No base Ketch	-	√
E16-5	-	√	√	286.12	-
E17-2	-	No URAN/POTA	√	223.23	√
E17-A2	-	√	√	217.54	-
KPK-01	-	No DT	No Caister SST	-	-

4 Methodology

Based on the available data, integrated stratigraphy in this study comprises biostratigraphy, Integrated Prediction Error Filter Analysis (INPEFA) stratigraphy, and lithostratigraphy (Fig. 4.1). The detailed biozones with a thickness of tens of meters to around 150 meters are in the intermediate scale. Two scales of the INPEFA approach are applied to extract medium-term trends and short-term trends. The medium-term INPEFA units range from tens of meters to approximately 150 meters in the vertical direction, and the short-term INPEFA units with a thickness of 7 to nearly 20 meters. The lithology correlation focuses on thick coal seams, as they can cover a large area in this study. The coal seams correlation is constrained by the biostratigraphy and INPEFA stratigraphy. The lateral extent of different stratigraphy, as well as cyclothem, will be analyzed and discussed through vertical well sections and lateral computed thickness maps.

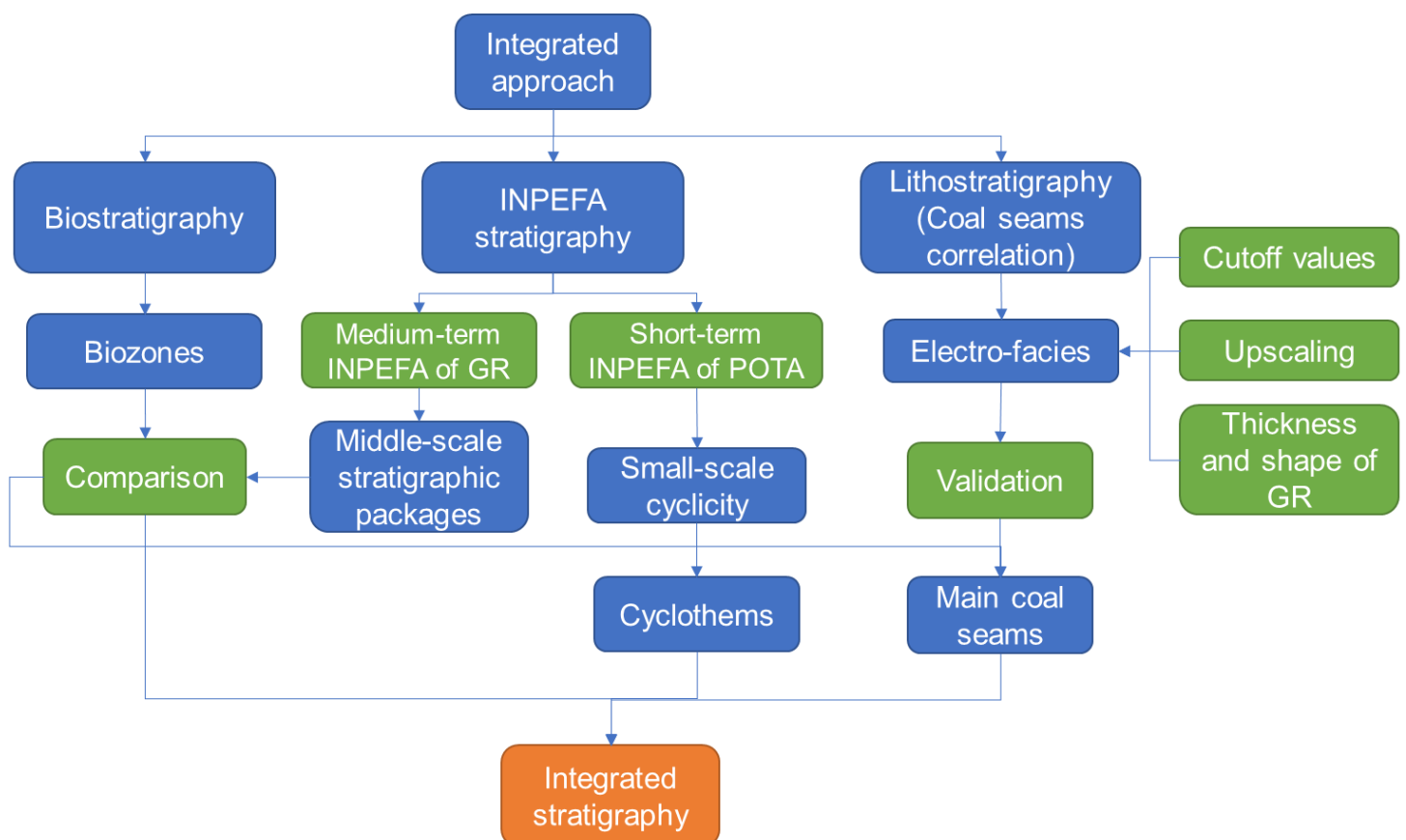


Fig. 4.1 The workflow of this study.

4.1. Electrofacies

As described in Chapter 2, deposits in the fluvial-deltaic system mainly consist of sandstone, siltstone, shale, and coals. Constrained by the wireline log data obtained from different companies without uniform standards, it's challenging to accurately distinguish sandstone and siltstone. Instead of detailed recognition of types of rock, different sedimentary facies associations will be identified. Thus, three general depositional facies which are sandstones, floodplain deposits (including shale and some siltstone) and coal seams will be interpreted. Then sandstones will be further classified according to the various sedimentary environment involving channels, point bars, crevasse splays, and mouth bars. The whole process will proceed in Python (Fig. 4.2). Also, it's challenging to accurately distinguish marine bands only based on wireline logs because different marine bands have various characteristics and log responses (Table. 4.1) (O'Mara, 1995). Thus, the marine bands that are commonly consisted of black shale are merged into the floodplain deposits type.

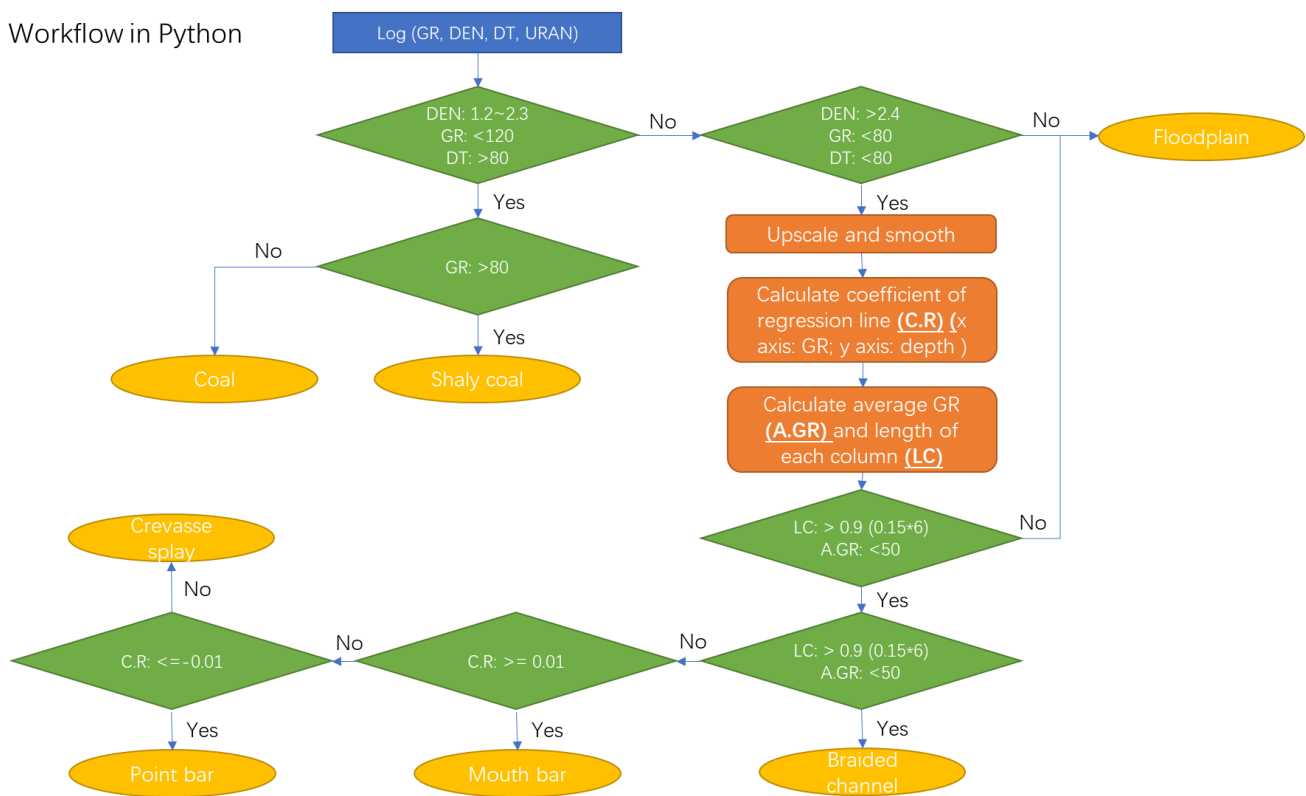


Fig. 4.2 Workflow for lithology and facies interpretation. The cutoff values are personally defined. They will be explained in Chapter 4 and shown in Chapter 5.

In terms of lithology, the usages of the various log are essential to know. Three types of petrophysical logs will be used for lithology identification: GR, DEN, and DT. The gamma ray log which can detect the radioactive isotopes is generally used to discriminate shales from other formations because the level of radiation in shales is usually high caused by the absorption of radioactive elements by clay minerals. By contrast, sandstones and coals have relatively lower GR values. The density log records the bulk density of

the rocks and it can be also useful in the identification of lithology though it runs primarily to estimate rock porosity. Whereas the density of coal can vary greatly due to different compaction ratios, the general density values of coals are lower compared to sandstone and limestone. The sonic log measures the speed of sound waves transmitting through rocks, which also can be used to indicate lithology. In general, moderate velocities are related to sandstones and low velocities are associated with coals.

Table. 4.1 Log responses of marine bands in Westphalian B stage in the southern North Sea. (modified from O'Mara (1995))

Marine bands	GR	URAN content	Characters
Aegiranum	High	High	Often eroded
Sutton	High	Slight high	Only known from the central part of the basin and in Northumberland
Haughton	High	Vary	Maybe inferred by the relative stratigraphic position of upper and lower marine bands
Clowne (Sub-Clowne tonstein)	High	High	Double gamma peak signal
Malby	High	High	Must be inferred from the Sub-Clown tonstein
Vanderbeckei	High	Low	Some variations in uranium response

In an overview, coals have moderate to low GR values, low DEN readings, and high DT values. Sandstone shows low GR readings, relatively high DEN values, and relatively low DT readings. Floodplain deposits have a wider range of petrophysical logging responses due to the complex composition including siltstone and shale. The distinctive feature of them is the high GR response, especially for marine shales. In order to automatically interpret them at a quick speed, cutoff values for lithology in the study area need to be set. The specific values will be defined based on 3D cross-plots of different lithologies which are interpreted manually and obtained from the Wintershall company, and literature researching on the similar depositional environment (Zhou B and O'Brien G, 2016; Zhou F, et al, 2020). The three coordinates are GR, DEN, DT, and the boundary values of different lithofacies units are expected to be different.

Based on the defined cutoff values, different lithologies including sandstone, shale, and coal at every logging sampling point can be identified. Logging vertical sampling interval is every 0.152 meters. In order to show concisely and in line with the common sense of sedimentary facies presentation, upscaling is applied to avoid thinly interspersed layers interpreted by cutoff values. The specific operation is to take each sampling point as the center and select the lithology with the highest frequency within a length of nearly 1 meter as the presentive lithology at that point. In other words, within each meter interval, the lithology with

the largest proportion will be used as the lithofacies for the entire section. But recognized coal seams will not be upscaled because coal seams are usually compacted to thin layers and they are essential to study the small-scale cyclothems.

As described in Chapter 1, sands can be subdivided in terms of different depositional environments. Braided channels, point bars, crevasse sands, and mouth bars are involved in this study (Fig. 4.3). The remarkable features of recognition of them from petrophysical logs are the shape and number of GR logs. Specifically, point bars that are fining-upward will show bell-shaped GR and the GR shape of mouth bars which are coarsening-upward is a funnel. Braided channels and crevasses usually show cylindrical GR while sands deposit in the major channel is usually coarser and thicker than sands deposit in crevasses (O'Mara, 1995; Kendall C, 2003). Hence, the GR log and depth regression line coefficient that can reflect changes in grain size and mean GR value of a column of sand deposits will be defined to further classify sedimentary facies of sands.

The calculation for the regression lines is shown in Eq. 4.1 and the best-fit slope m is shown in Eq. 4.2.

$$y = mx + b \text{ (Eq. 4.1)}$$

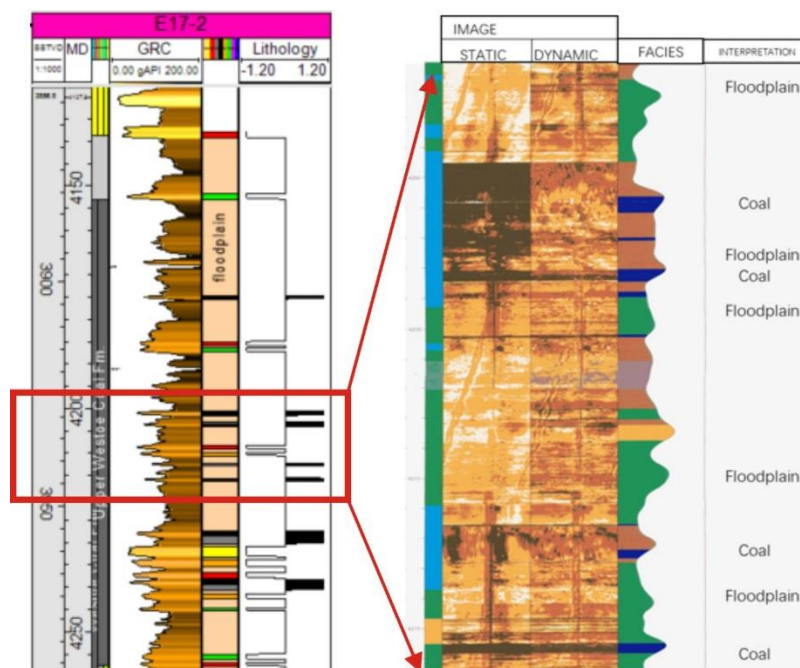
$$m = ((\text{mean}(x) * \text{mean}(y)) - \text{mean}(x * y)) / ((\text{mean}(x) * \text{mean}(x)) - \text{mean}(x * x)) \text{ (Eq. 4.2)}$$

where x represents GR values and y is depth. If a column of sandy deposits is coarsening upward showing funnel shape, the GR values increases as the depth increases, and then the best-fit coefficient is positive and vice versa.

Facies association	Core Profile Silt F M Crs	Gamma Ray 0 120	Description (schematic diagram of regression curve)
Point bar			Bell shape; Fining-upward
Mouth bar			Funnel shape; Coarsening-upward
Crevasse			Serrate shape; Medium-grained
Braided channel			Serrate shape; Coarse-grained; Thick (can reach 20 m)

Fig. 4.3 Summary of typical sandstone facies associations in Westphalian B in the study area and corresponding log response characteristics. The classification of facies associations and the core profile were modified from O'Mara (1995).

Core materials and reports are used to evaluate the interpreted electrofacies, especially coal seams. By comparing the location of specific electrofacies like coals to the position of the same lithofacies in the cores with the consideration of depth-shift between wireline log and cores, the accuracy of the electrofacies can be calculated (Fig. 4.4). To be more specific, the depth of coal recognized from core columns and the depth of coal electrofacies need to be recorded. Then, the depth shift can be calculated by comparing the depth of two records. Also, the total thickness of coal eletrofacies can be counted and divided by the total thickness of coals identified from cores to get the coverage of eletrofacies. Six wells will be used to validate the reliability of the automatically interpreted electrofacies. They are Well 44/22-4, Well 44/23-6, Well 44/28-2, Well 44/28-3, Well E16-3, and Well E17-2.



Or



Electrofacies:
■ Channel ■ Point bar ■ Mouth bar ■ Crevasse
■ Floodplain ■ Coal ■ Shaly coal

Lithology:
-1: SANDS;
0: FLOODPLAIN;
1: COALS

Fig. 4.4 The processes of evaluation of electrofacies. Core materials or FMI data are used to compare.

4.2. Biostratigraphy

Offshore biozones are defined based on the last occurrences of zonal taxa. Due to the scarcity of core coverage, core-cuttings materials are used. The regional taxa with stratigraphically significance are selected based on the consistent appearance from top to bottom in well sections and the representation compared to the onshore biozones.

The definition and division of different biozones that developed in the Westphalian stage used in this study are derived from McLean et al (2005). The biozones data is derived from bio-reports available on the NDR (https://ndr.ogauthority.co.uk/dp/controller/PLEASE_LOGIN_PAGE) and recent work from Huis In't Veld (personal communication, 2021). This study focuses on summarizing these intervals, correlating and comparing them. A convergent interpolation method is applied to 2D map generation by using the vertical division in wells. Consequently, the lateral consistency and heterogeneity of each biozone can be analyzed by combing the thickness distribution in the study area.

4.3. INPEFA stratigraphy

The INPEFA is good to extract unseen visual information from the wireline log and used to identify discontinuities, depositional trends, and hierarchical patterns in the stratigraphic succession. Especially when it is applied to facies sensitive logging data, it could reflect vertical lithofacies changes and identical patterns (De Jong et al, 2020). Besides, the sedimentary cycles could also be extracted by using INPEFA (De Jong et al, 2020; Yong H et al, 2021).

Before calculating the integrated prediction error, an L1 trend filtering proposed by Kim et al. (2009) is used, as it is a powerful tool to estimate a piecewise linear trend without priorly defining the position and number of kink points (Kim, 2009; Hiroshi Yamada and Gawon Yoon, 2015). This is very similar to the situation in this study. The potential cycles may exist in the subsurface and be recorded by lithofacies-sensitive logging curves, but the specific turning points are unknown.

Afterward, another mathematical method named Maximum Entropy Spectral Analysis (MESA) (Burg, 1967) is applied. By using a sliding window with a given length, MESA is able to calculate a Prediction Error Filter

(PEFA), an expression of the errors arising from the prediction of data from one window to the next. It shows the continuity of the waveform of the signals. The mathematic expression is regarded as :

$$e_i = x_i - \hat{x}_i = x_i - \sum_{k=1}^m \alpha_k x_{i-k}, i = m + 1, \dots, N. \text{ (Eq. 4.3)}$$

where x_i denotes the real log value and \hat{x}_i is the prediction value from the autoregressive model (Bos, 1971). Besides, α_k represents the filtering factor, N is the length of the window and e_i is the output of the filter. The integration of PEFA is INPEFA that can indicate the cumulative errors during prediction and reflect the spectral trend attribute (Nio et al. 2005; Yong H et al, 2021).

Some types of wireline logs such as spectrum gamma-ray are good indicators of lithologies that are related to sedimentary successions. The GR log is sensitive to the facies and the potassium component (POTA) of the GR log is associated with feldspar content. This is one type of clay mineral and, thus, the spectral change of GR and POTA logs derived by INPEFA can indicate important stratigraphic breaks and changes in the sedimentary environment. In other words, it's crucial for lithofacies patterns and sedimentary cycle research to study the turning points and the trends (Nio et al., 2005; Yong H et al, 2021).

The INPEFA curves are standardized to values between -1 and 1. The intervals in the INPEFA curve are separated by turning points (Fig. 4.5). A positive turning point indicates a trend changing from negative to positive in an upward direction and a negative turning point reflects a trend changing from positive to negative from bottom to top. Typical positive turning points are generally regarded as the base of progradational successions and manifest negative turning points are usually considered as the beginning of retrogradation processes (Nio et al., 2005; De Jong et al., 2007).

Considering the potential intermediate-scale cyclicity with the thickness of tens of meters, and small-scale cyclothem developed in the study interval, different filters of INPEFA will be experienced on GR and POTA log and compared, aiming at extracting these two scales of trends. The INPEFA curves with the most visible cyclicity will be selected as act the final results. The matched patterns should be enveloped resembling C-shape from INPEFA curves with specific lengths. The interval in terms of medium-term cyclicity is also called the stratigraphic package (De Jong et al., 2020). 2D map created by convergent interpolation method and thickness distribution will also be applied to study the lateral extent of each cycle.

The stratigraphic packages are thought to be time-synchronous and climate-controlled (Nio, 2008; De Jong et al., 2007). The astronomical forcing will also be discussed in the present study by comparing the thickness of each cycle and counting the number of the short-term cycles extracted from INPEFA as well as comparing medium-term INPEFA cycles with biozones which are thought to be time-equivalent.

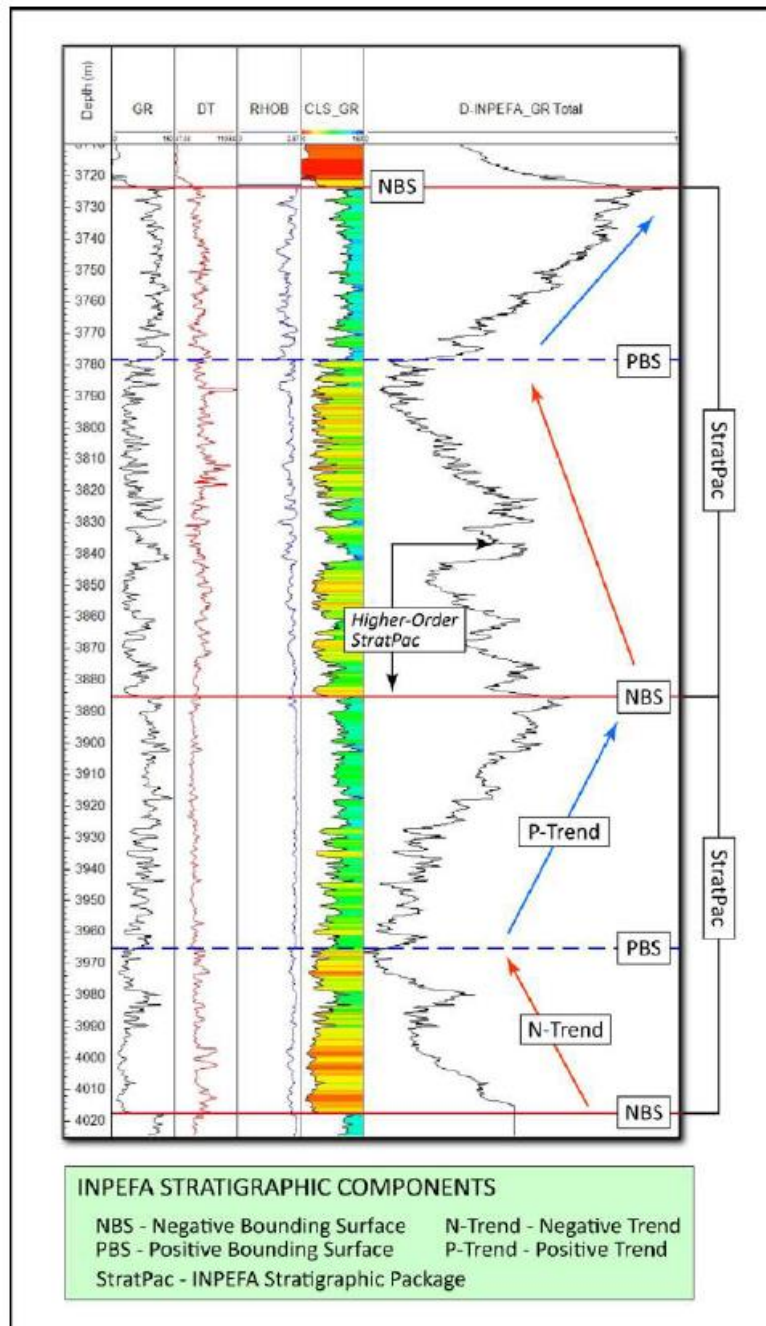


Fig. 4.5 Components of INPEFA stratigraphy (from ENRES international open report, 2011). NBS and PBS are the surfaces where negative turning points and positive turning points occur.

4.4. Lithostratigraphy

To better show the distribution of lithofacies in the well sections, different codes are given to three main lithofacies. Sands recognized from electrofacies are set as -1. Floodplain deposits which are the most

developed in the whole interval are provided to 0. And the coal seams that have the largest potential to correlate are given 1.

The correlation of lithology is concentrated on coal seams which are remarkable, with the consideration of trend changes of different grain-sized lithologies. With a low-relief slope, some flooding events including marine incursions could cover the entire region of interest and form coal seams or marine bands. The zonation of correlation of coal seams relies on distinctive log responses, especially URAN and URAN/THOR, and the constrain from intermediate-scale zones divided by biostratigraphy or INPEFA stratigraphy.

Due to the long well-to-well distance usually reaching several kilometers, the direct correlation of channel sands is unreliable. The distance between the study wells is long, usually ranging from a few kilometers to more than ten kilometers, which far exceeds the width of the channel belt. It is challenging to connect the same channel sands on the regional scale only based on the interpreted lithofacies.

The identification of marine bands based on the wireline logs is not acceptable in all wells as a result of the heterogeneous character of different marine bands (O'Mara, 1995). Furthermore, the marine bands have been taken into account during the classification of biozones (McLean et al., 2005). Therefore, the correlation of marine bands is excluded. Nevertheless, the relative position of sand bodies with marine bands and coal seams in the vertical direction will be considered during zonation and correlation of trend changes. The correlation of the fifth-order cyclothems will be attempted in several wells about three to four kilometers away. Afterwards, the lateral extent of cyclothems and different facies can be discussed.

5 Results

5.1. Electrofacies

Three general lithofacies in the study area are sands, coals, and floodplain deposits. The cutoff values of GR, DEN, and AC for three lithofacies (Table. 5.1) are set based on the 3D cross-plot (Fig. 5.1) of different lithologies interpreted by the Wintershall company and a study in the nearby area (Bosch, 2008). Note that the three conditions of the logging threshold need to be met at the same time. There are some overlaps between the values of the three lithologies (Fig. 5.1). Thus, further validation of automatic interpretation, especially the coverage of the results is needed.

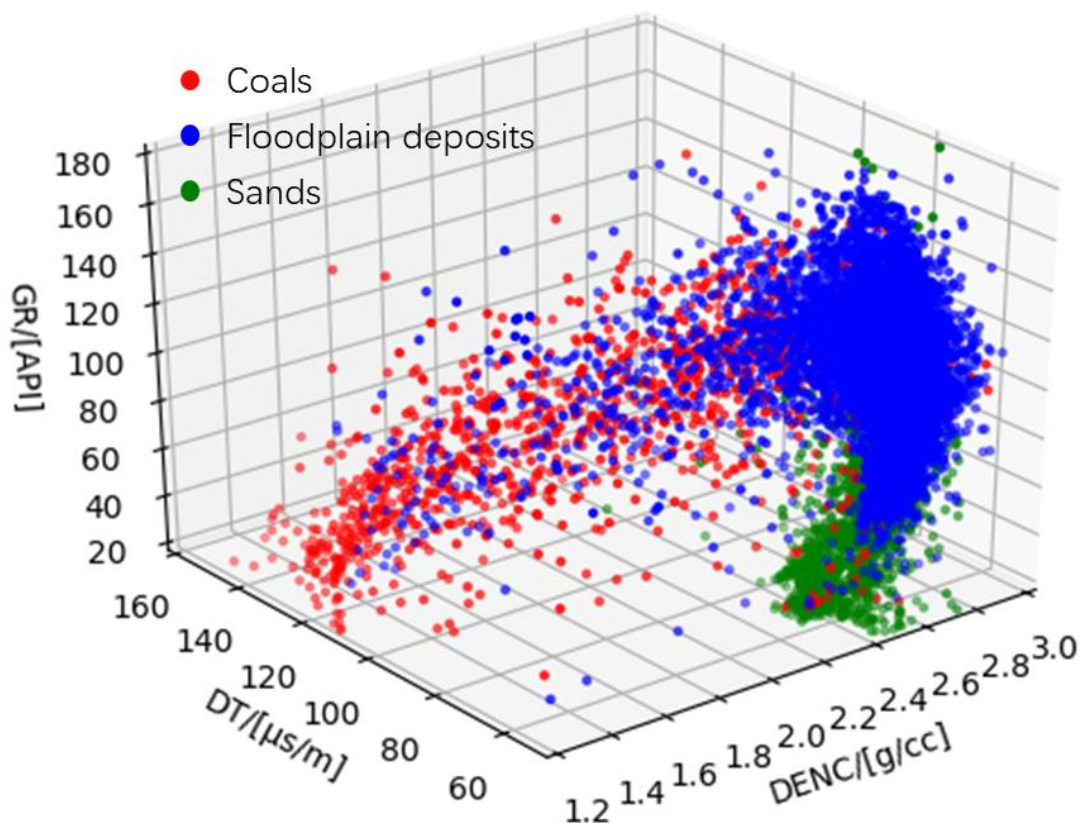


Fig. 5.1 3D cross plots of DEN, DT, and GR logs of different lithologies. Red points represent coals; blue points indicate floodplain deposits; green points stand for sands.

The coals are generally characterized by low GR which is usually lower than 80 API (Binzhong Zhou and Graham O'Brien, 2015). But coal seams in the study area sometimes have high GR which is nearly 120

API. The high GR response results from the high shale content (Pradier and Nicolas, 1995). The coal seams were deposited in a low-relief swampy area where floodplain deposits dominated, and the coals were possible correlatable regional flooding events. In terms of water table level, the humidity of depositional setting of coal seams differs and the vegetation, as well as sediments input, were various, resulting in different shale content in coal seams. Thus, two types of coal seams are differentiated in this study; normal coal seams and shaly coal seams. The cutoff value of GR is 80 API for both coal types.

Table. 5.1 Defined cutoff values for different lithologies in the study area.

Lithofacies	Sands	Coal	Floodplain deposits
GR, API	<80	<120	Rest
DEN, g/cc	>2.4	1.2~2.3	Rest
AC, $\mu\text{s/m}$	<80	>80	Rest

The further cutoff values for sandy deposits are defined according to the shape and the mean value of GR (Table. 5.2). Considering the possible noise and errors in logging data, the cutoff range of GR for cylindrical shape is set from -0.01 to 0.01 instead of cutoff values equal to 0. The minor channels in the study area typically consist of 2.5 m sandstone and the channel fills are generally medium- to coarse-grained sandstones (O'Mara, 1995). The crevasse deposits mainly compose fine-grained sandstone but also were filled with silty partings (O'Mara, 1995). Considering that the sampling interval of wireline logs in this study is equal to 0.152 m, the thickness of channels is set to be greater than 2.4 m and the mean GR value is lower than 50 API.

Table. 5.2 Defined cutoff values for different facies of sandy deposits.

Sedimentary facies	Channels	Crevasse	Point bars	Mouth bars
Thickness, m	>2.4	-	-	-
Coefficients	-0.01~0.01	-0.01~0.01	<-0.01	>0.01
Mean GR, API	<50	-	-	-

As a result, seven sedimentary facies associations are defined. These facies associations, which are channel, crevasse, point bar, mouth bar, floodplain, coal, shaly coal, and floodplain, are plotted for all wells in this study (Fig. 5.2).

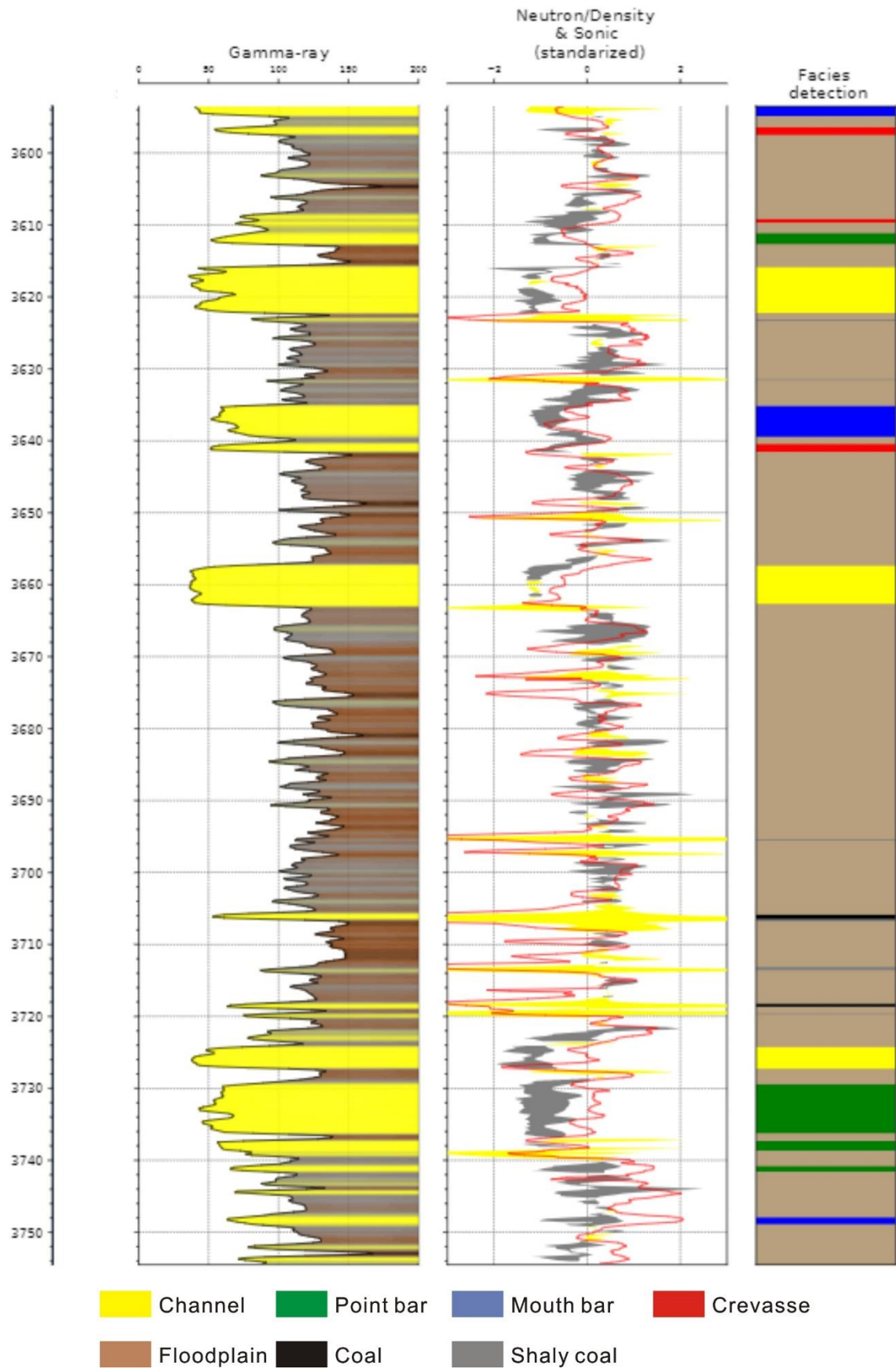


Fig. 5.2 Automatically interpreted electrofacies (last column) of Well 44/12a-3. The first column represents measured depth. The second column shows GR and the fourth column contains DEN, NPHI, and DT. In the

third column, the yellow area indicates that NPHI is larger than DEN and the grey area represents that DEN is larger than NPHI. Seven facies associations are interpreted based on these log data.

The study interval is much thicker in the southern area than in the northern part. The total thickness of the succession is nearly 170 m in the north and around 700 m in the south. In the Westoe Coal formation and Cleaver formation, the floodplain deposits cover a large proportion which is around 76.4%, and sandstone sediments account for nearly 18.2% (Fig. 5.3). The depicted net-to-gross ratio is around 20% in the whole succession. The net-to-gross ratio is higher in the Cleaver formation which is equal to 25.8% compared to the net-to-gross ratio in the Westoe Coal formation which is equal to 17% (Appendix A). Channel sands also rarely appear in the Westoe Coal formation compared to Cleaver formation, after the deposition of Caister sandstone. Specifically, channel sands occupy 11.2% in the Cleaver formation and only 4.5% in the Westoe Coal formation (Appendix A). The overall thickness of the coal seams becomes thicker from north to south, ranging from a few meters to nearly 30 m. Individual thick coal seams with 2 to 3 meters thickness are more frequently recognized from wells in the southern area. The thickness of individual coal seams in the northern part is usually thinner than 1 m.

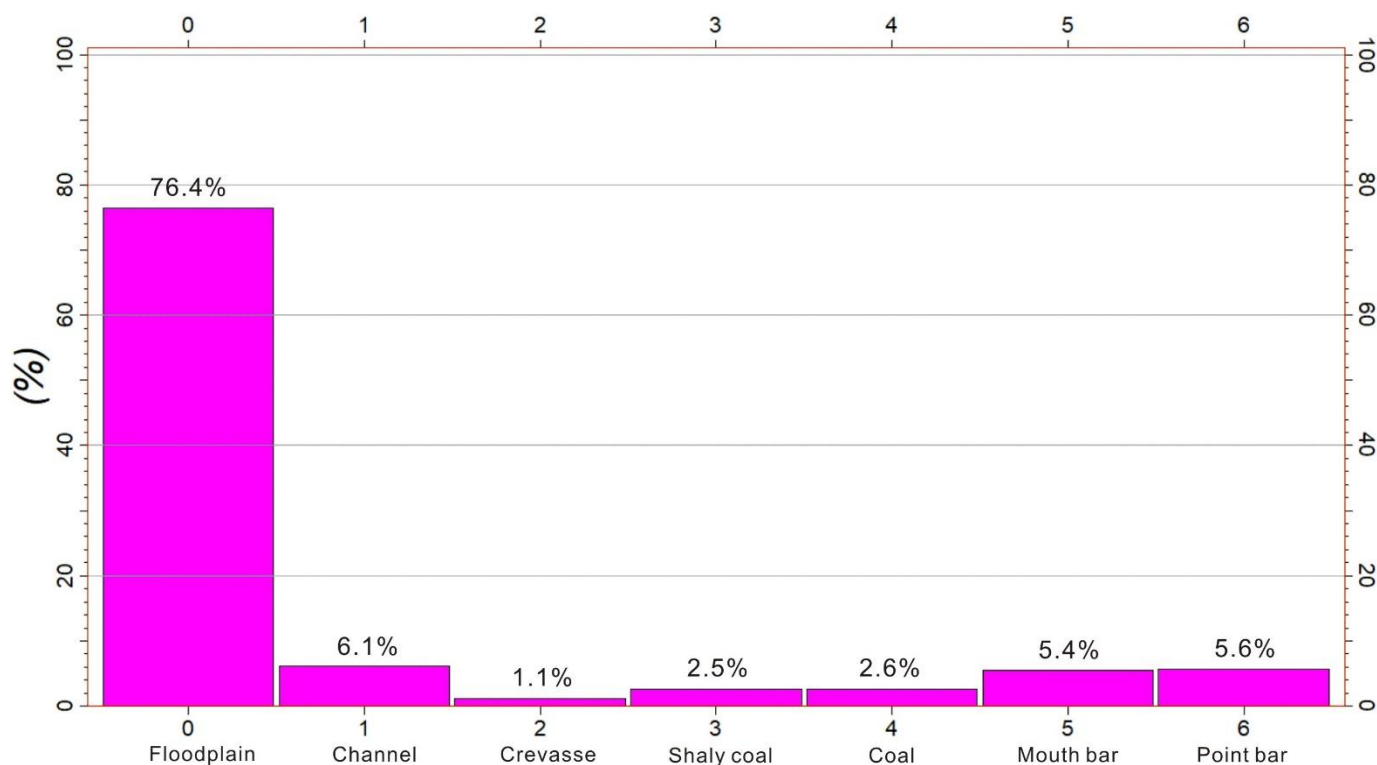


Fig. 5.3 Histogram of the percentage of different electrofacies in 25 wells of the study area combined. Note that marine bands are incorporated in the 'floodplain' electrofacies because of recognition difficulties

Six wells with core materials or FMI data are used to validate the electrofacies, especially for coal seams (Fig. 5.4). The depth of coal seams recognized in the core columns is compared to the depth of the coal electrofacies. The coverage of coal electroface compared to the coals interpreted from core materials can be calculated (Table. 5.3). And the depth shift of each coal seam between core materials and the wireline logs

can be obtained by comparing their depositional patterns (Table. 5.3). Note that only core materials of Well E17-2 cover the whole interval. Other used core materials and FMI data occupy part of the study successions.

Based on the comparison results (Table. 5.3), the thick coal seams can be well identified by electrofacies. But some thin coal seams usually thinner than 0.2 m cannot be recognized. This is due to the vertical sampling resolution of logging data. The coverage of coal seams electroface is more than 70% and the depth shift between cores and the wireline logs is limited to 8 meters (Table. 5.3). This indicates that the interpreted electrofacies are acceptable and can be used in the following study.

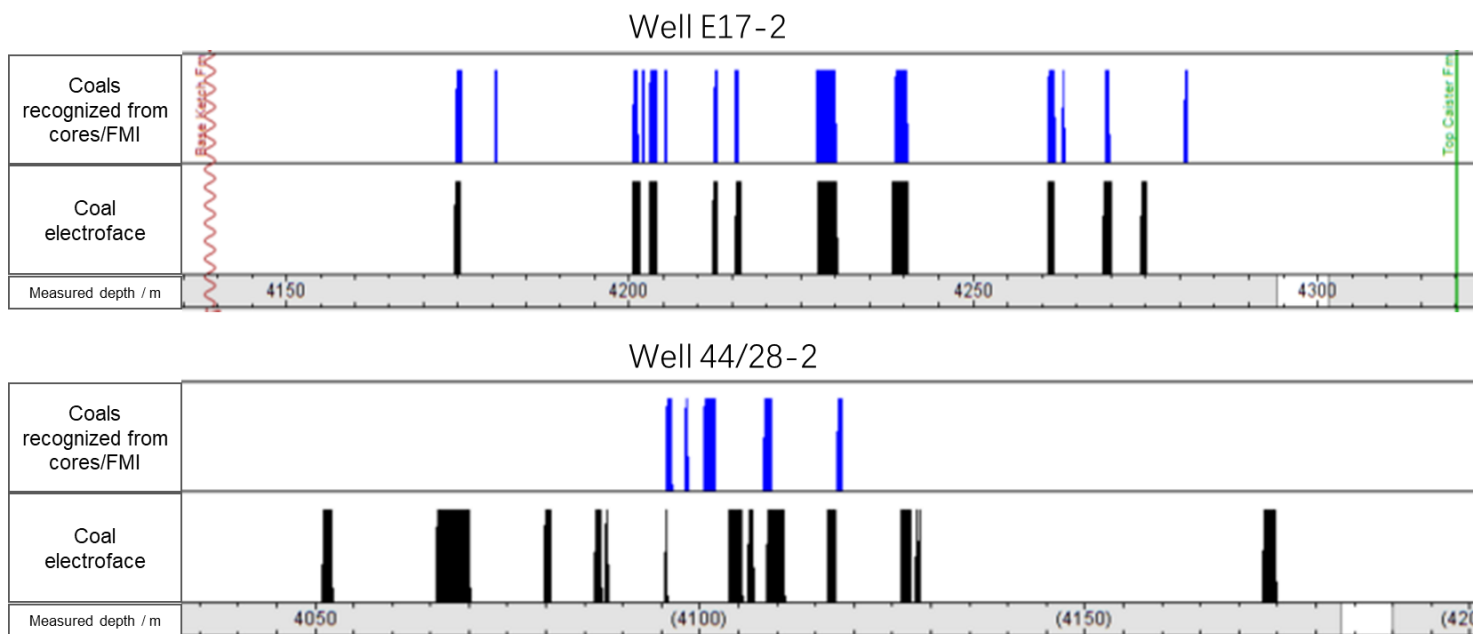


Fig. 5.4 Comparison between coals recognized from cores/ FMI and coals identified from logging data. Two wells, namely E17-2 and 44/28-2 from different quadrants are set as examples of the validation. Note that the core materials of Well 44/28-2 do not cover the whole study interval.

Table. 5.3 Evaluation of the coverage of coal seams electrofacies and the depth shift between cores and wireline logs.

Well	44/22-4	44/23-6	44/28-2	44/28-3	E16-3	E17-2
Coverage	100%	70%	84.40%	91.74%	90.80%	87.24%
Depth shift	0.5m	0.2m	0.5-8m	≈3m	3-5m	0.5-1m

5.2. Biostratigraphy

There are a total of six biozones defined, namely W4a, W4b, W4c/d, W5a, W5b, W6a. Not all biozones were found in each well (Fig. 5.5, Fig. 5.6). The northernmost well 44/12a-3 has W4a and W4b biozones while the southernmost well 49/2-3 has all six biozones from W4a to W6a. The W4a and W4b biozones that are located at the bottom cover the whole study area. Starting from the W4c/d interval and upward, biozones gradually disappear in the northern area, and they can not be traced until they extend to the middle area. The top W5b and W6a biozones only cover the southern part. The biostratigraphy is relatively consistent in the east-west direction. Note that the Cleaver formation in some wells like 44/12a-3 is excluded from these six biozones. They are in the same biozone of the Ketch formation overlying the Cleaver formation. It also indicates that the classified formations are diachronous.

The thickness of each biozone varies and the trend of change also differs (Fig. 5.5, Appendix B). W4a is thicker in the southwest area and thinner in the northeast part. Especially at the location of Well 44/27-1, the thickness of W4a can reach around 140 m. W4b biozone has similar features. The thickest W4b zone that is nearly 150 m is found in the Well 49/2-3 located in the south. And the thickness of W4b in the north area is closed to 40 m. W4c/d becomes thicker from north to south. However, it cannot be traced in the northernmost Well 44/12a-3. The thickness of W4c/d in the northern part ranges from 0 to 30 m. The consistency of W4c/d is good in the central and southern parts and the variation of the thickness between wells in these two areas is less than 30 m. W5a gradually thins from west to east. It can only be traced in the central and southern areas. The thickest W5a which is nearly 65 m is found in the Well 44/21a-7. The top zones W5b and W6a only cover a small area in the south and tend to thicken towards the south. These top two zones were only found in three wells which are W44/27-1, W44/28-2, and Well 49/2-3.

It should be noted that the thickness trend depends on the resolution of biozones definition by specific miospore taxa, and it is affected by the uncertainty of the data. The primary locations of the palynological assemblages could be changed during drilling, and the measured depth could not be very accurate. Hence, the boundaries of biozones are not solid surfaces.

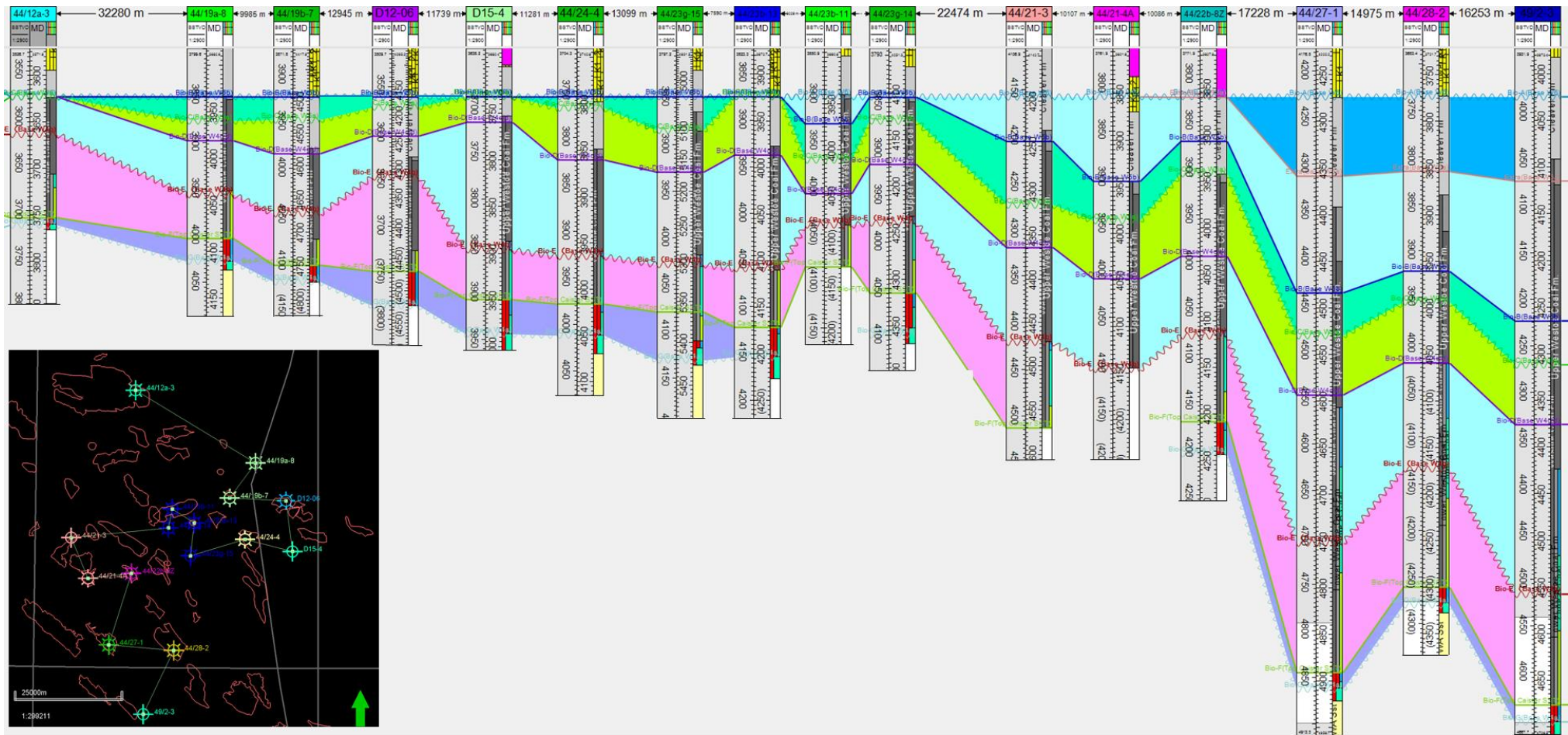


Fig. 5.5 Long-distance correlation of biostratigraphy. The wells are situated in Quadrant 44, 49, and D, extending from north to south. From bottom to top, the purple zone denotes the Caister sandstone interval; the purple and pink zones represent W4a; the light-blue zone located in the lower succession is W4b; the yellow zone represents W4c/d; the green zone denotes W5a. The top two zones are W5b and W6a, respectively.

5.3. INPEFA stratigraphy

INPEFA curves of GR are generated for 16 wells with complete study interval (Table. 3.2) and INPEFA curves of POTA are created for wells that have Pota logs (Table. 3.2). Using turning points and turning surfaces in the INPEFA curves, different scales of units can be recognized. In this study, intermediate-scale stratigraphic packages with a thickness of tens of meters to 150 m are classified from medium-term INPEFA curves of GR. Small-scale cycles ranging from 7 to around 20 m are identified from short-term INPEFA curves of POTA.

5.3.1 Medium-term INPEFA of GR

Six stratigraphic packages are classified from medium-term INPEFA curves of GR by strong negative turning points, showing C-shape (Fig. 5.6). The value of strong negative turning points generally is larger than 0.8. Commonly, the boundaries that are the negative turning surfaces are the basis of sandstone successions including channel sands, point bars, and mouth bars. The thickness of the stratigraphic packages ranges from tens of meters to around 150 m. In each stratigraphic package, the sand content decreases upwards, from about 35% to around 5%. Coherent with this, the floodplain deposits become abundant at the top of each package. Also, coal seams usually more frequently appear in the upper part of stratigraphic packages.

From bottom to top, the stratigraphic packages are named IG1, IG2, IG3, IG4, IG5, and IG6 (Fig. 5.6). Not all stratigraphic packages can be traced in each well (Fig. 5.7). The bottom three zones IG1, IG2, and IG3 cover the whole study area. IG4 can extend to the central part but cannot be traced to the northern area. The top two zones IG5 and IG6 only develop in the southern area. Specifically, the northernmost Well 44/12a-3 only has three stratigraphic packages, namely IG1, IG2, and IG3, while the southernmost Well 49/2-3 contains the most complete stratigraphic packages in the study area. Note that the Cleaver formation in all wells is involved during the classification of stratigraphic packages.

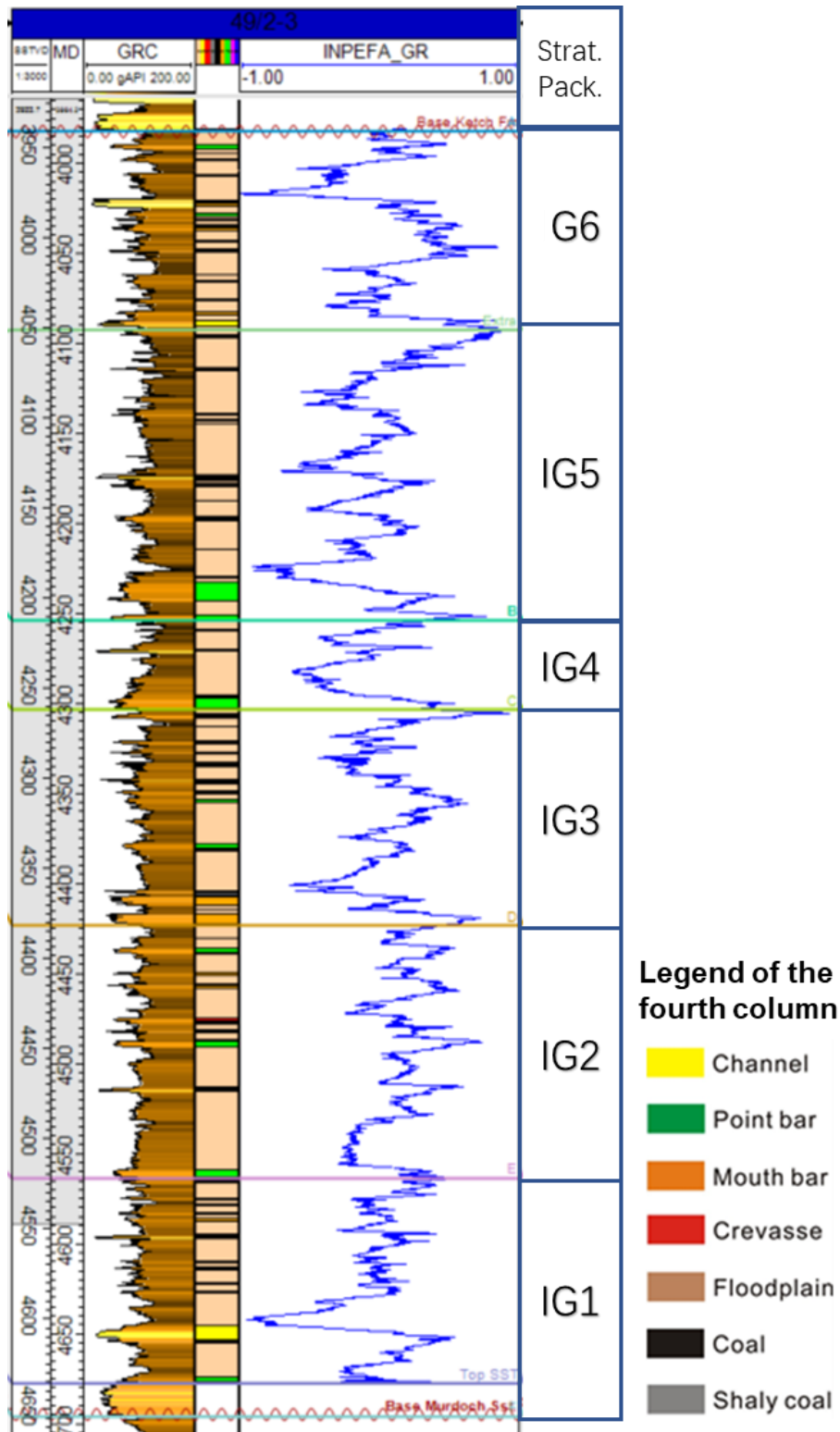


Fig. 5.6 Result of INPEFA of GR curve with the divided stratigraphic packages in Well 49/2-3. The first column is true vertical depth. The second column represents measured depth. The third column is the GR log, and the fourth column is the interpreted eletrofacies. The fifth column is the medium-term INPEFA of GR. The last column indicates the identified stratigraphic packages based upon strong negative turning points.

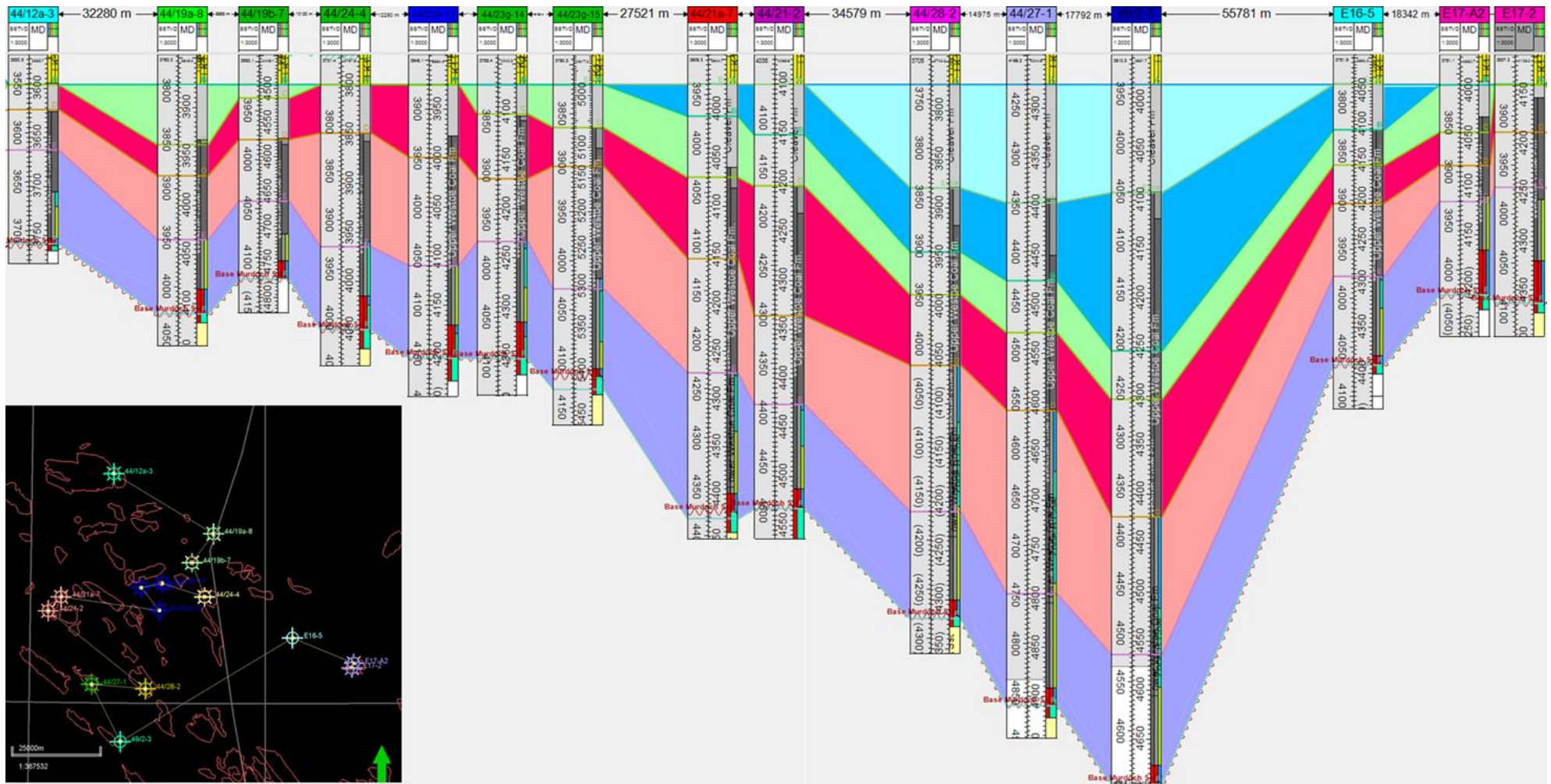


Fig. 5.7 Long-distance correlation of INPEFFA stratigraphy. The wells are situated in Quadrant 44, 49, and E, extending from north to south. The purple zone denotes IG1; the pink zone represents IG2; the red zone is IG3; the green zone represents IG4. The top two zones are IG5 and IG6, respectively.

Each stratigraphic package has a variable thickness, and the thickness of different stratigraphic packages also varies a lot between wells (Fig. 5.7, Appendix C). From an overall view, the two bottom stratigraphic packages, IG1 and IG2 are thicker than the other stratigraphic packages. Most intervals of IG1 and IG2 exceed 50 m and can reach 150 m in some wells located in the south and west areas. The middle IG4 and IG5 are the thinnest intervals. For IG1, IG2, and IG3, the thinnest part is situated in the northeast area and they are thicker in the southwest. But the thickest IG1 appears in the west area, especially at the location of Well 44/21a-7. IG4 also becomes thicker from northeast to southwest, but it is absent in the north part of the study area. IG5 and IG6 can only be traced in the southern area. IG5 becomes thicker from northwest to southeast while IG6 thickens from southwest to northeast.

5.3.2 Comparison between Biozones and INPEFA stratigraphic packages

The biozones and INPEFA stratigraphic packages match each other, though a small offset exists (Table 5.4 and Fig. 5.8). The lower three zones which are W4a, W4b, W4c in biostratigraphy and IG1, IG2, IG3 in INPEFA stratigraphic packages are more lateral extent in the whole study area. They are generally thicker in the southern part and thinner in the northern areas. The stratigraphic package IG4 is absent in the north, which is in line with the biozone W5a. The top two units that are IG5, IG6 in INPEFA stratigraphy and W5b, W6a in biostratigraphy can only be traced in the southern area. The W4a and IG1 is the best-correlated interval located at the bottom. The offset is limited to 30 m. Starting from IG2 and going up, the difference of depth of bounding surfaces between the two stratigraphic markers gradually increases, especially for the northern area and Quadrant D. Nevertheless, the offset of bounding surfaces between the two types of zonation is around 2 to 15 m, with the biggest offset around 60 m. Compared with the scale of the divided intervals, this depth shift is relatively smaller and acceptable.

The reason why the uppermost boundary of the two approaches is different is that the whole Cleaver formation is included in the classification of the INPEFA stratigraphic package, which is not the case for biozonation. The definition of formation which belongs to lithostratigraphy is diachronous. Without the Aegiranum marine band which is often eroded, the timeline of two depositional stages which are Westphalian B and C is hard to determine.

Table. 5.4 Correspondence between the two types of intervals.

Bio-surface	Bio_A (Base W6)	Extra (Base W6a)	Bio_B (Base W5b)	Bio_C (Base W5a)	Bio_D (Base W4c)	Bio_E (Base W4b)	Bio_F (Top SST)	Bio_G (Base W4a)
Biozones	W6a	W5b	W5a	W4c	W4b	W4a		
INPEFA	A	Extra	B	C	D	E	Top SST	F
Strat.Pack	IG6	IG5	IG4	IG3	IG2	IG1		

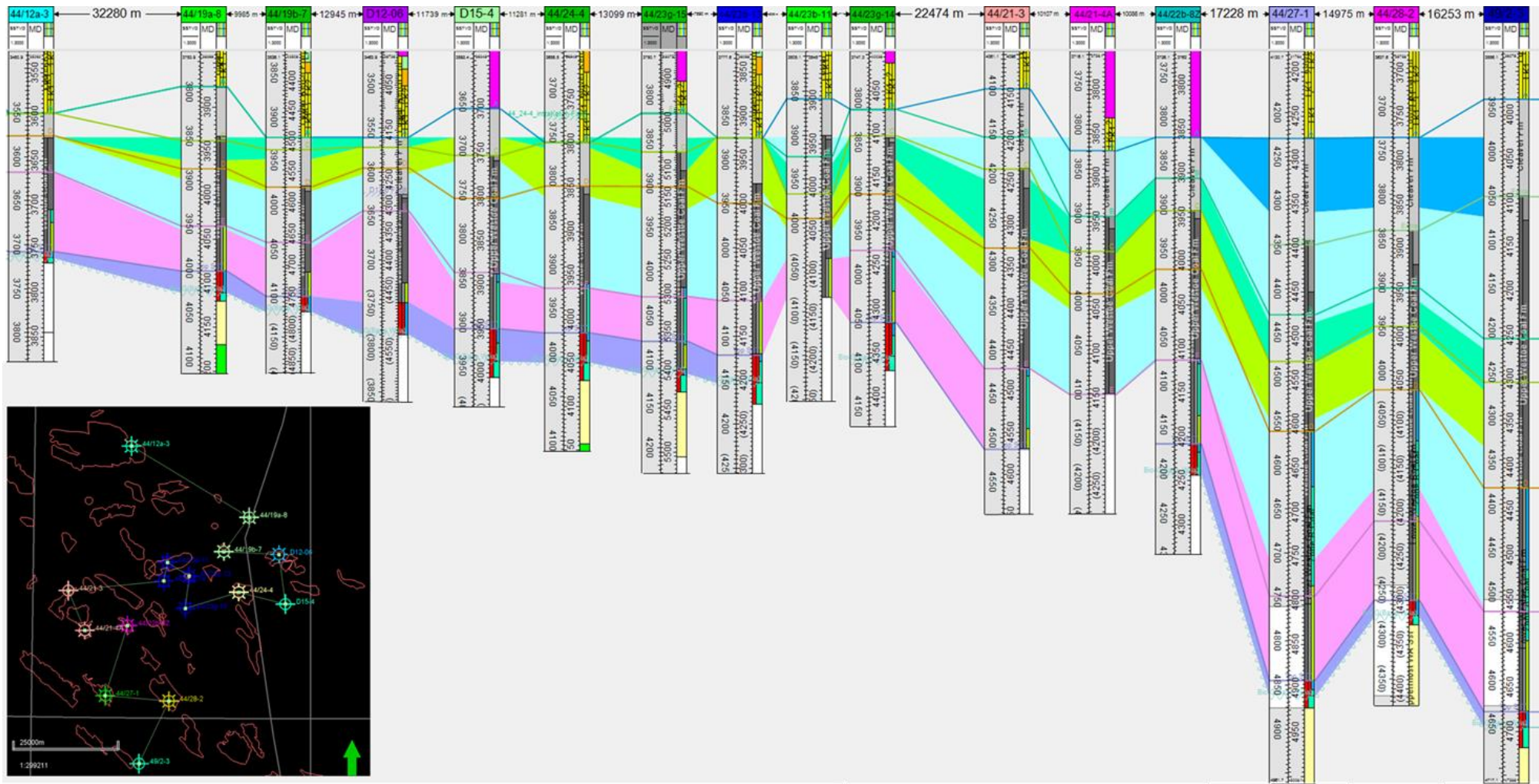


Fig. 5.8 Comparison between biostratigraphy and INPEFA stratigraphy. The background color represents biozones and the lines denote the INPEFA stratigraphy.

5.3.3 Short-term INPEFA of POTA

Small-scale cycles ranging from 7 m to 20 m are identified from short-term INPEFA of POTA in many wells, especially in the wells situated in the southern part (Fig. 5.9). Typical cycles are characterized by two positive turning points and a tendency to increase first and then decrease from bottom to top (Fig. 5.9). They show a C-shape. However, not all cycles show a perfect C-shape, which increases the difficulty of number counting.

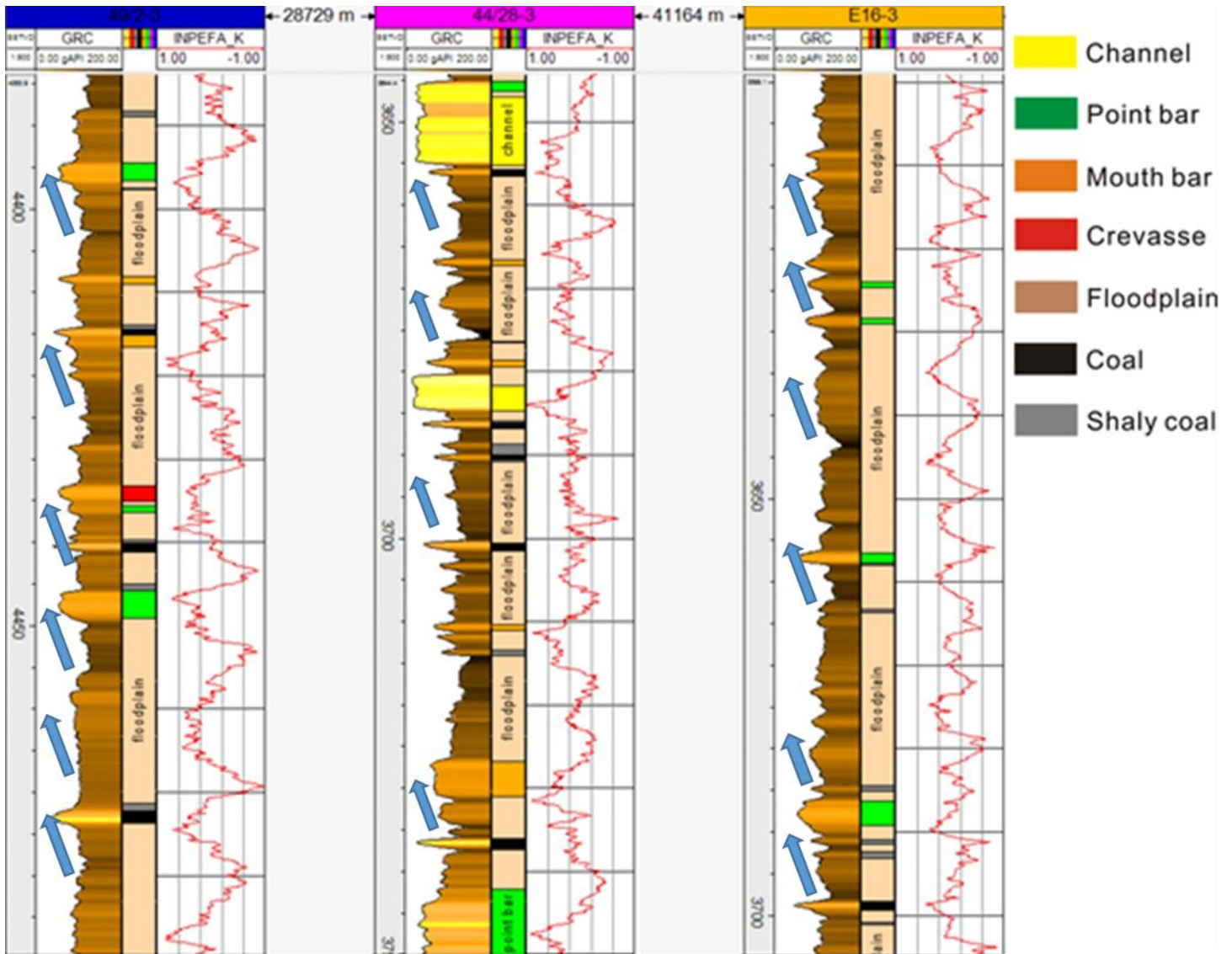


Fig. 5.9 Results of short-term INPEFA curves of POTA (last column). Small-scale cycles are visible. The first column is true vertical depth. The second column represents the GR log, and the third column denotes the electrofacies interpreted in this study.

Considering the uncertainty resulting from the less well-developed cycles, three different standards are set to count the number and calculate the average thickness: (1) the most cycles defined by every positive turning point and the smallest average thickness; (2) the minimum cycles separated by positive turning

points with the minimum values which is commonly -0.6 and the thickest average thickness; (3) the most likely cycles based on the observation of GR shape and the corresponding thickness (Fig. 5.10). The average thickness and the number of short-term INPEFA cycles are variable in each well. Well 49/2-3 and Well 49/3-1 contain the most cycles that are approximately 55 over the whole target interval. Well 44/12a-3 that is the most northern well has only 16 cycles. The cycles in the southern area are relatively thicker than the cycles in the northern area. The cycles developed in Quadrant D and E are the thinnest. The variation between the maximum average thickness and minimum average thickness of cycles shows large in the northern and central wells where less well-developed cycles occur.

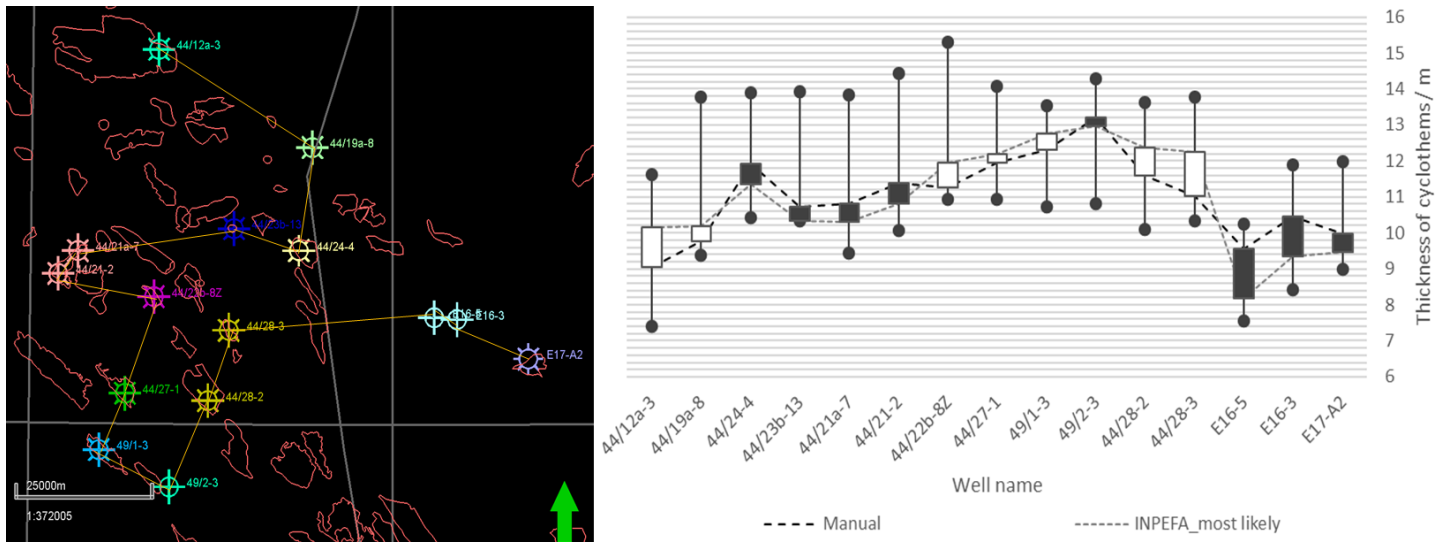


Fig. 5.10 Average thickness of cycles identified by short-term INPEFA curve of POTA and manual interpretation of cyclothem based on GR is shown in the right figure, and the figure of locations of wells is left. Note that the range of average thickness of cycles recognized by INPEFA curves is calculated by maximum and minimum numbers, and it is marked by a black line with two points. The blocks indicate the difference between the most likely average thickness of cycles according to INPEFA and the average thickness of defined cyclothem.

5.4. Coal seams correlation

The distribution of coal seams is greatly variable in the studied area, raising the difficulty of making a correlation of coal seams. Thicker and denser coal seams are deposited in the south, while the coal seams in the north and Quadrant D are thin and sometimes almost invisible. In this way, if the distance between adjacent wells does not exceed roughly 5 km, the connection of a single coal seam seems feasible, but it is not easy to proceed with the increasing well spacing.

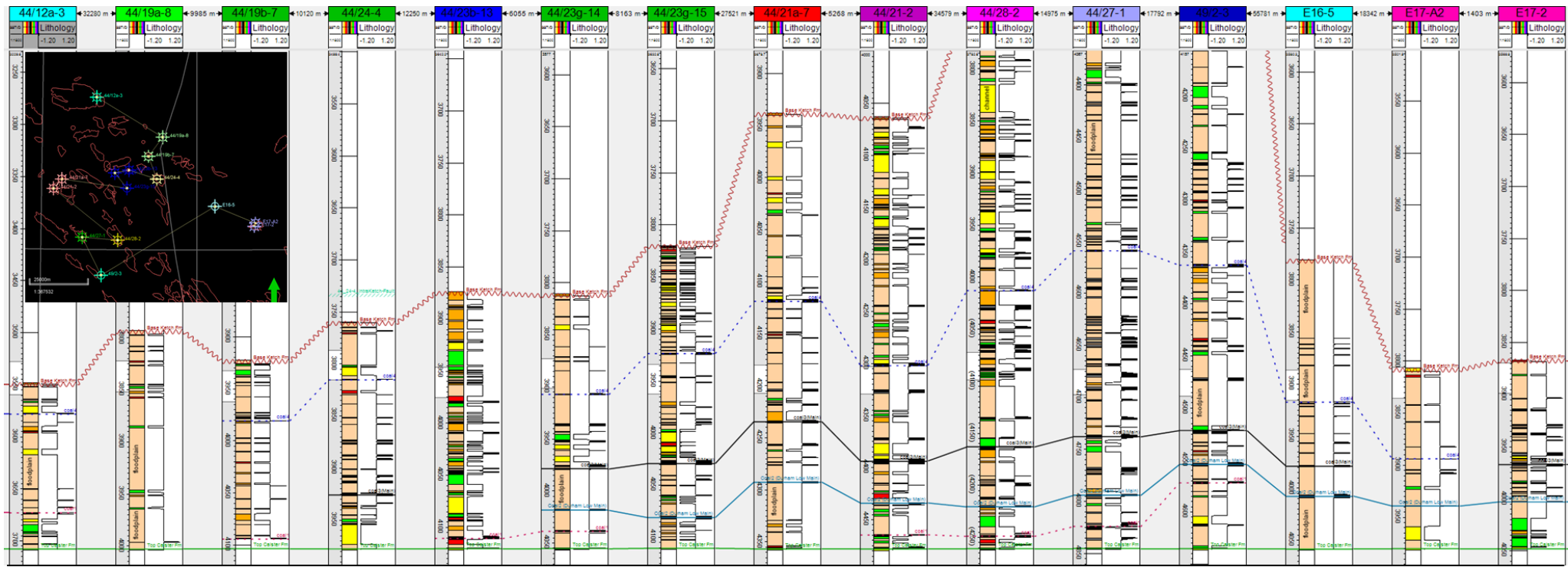


Fig. 5.11 Long-distance correlation of main coal seams. The dashed line colored in red, located at the bottom denotes Coal 1. The light blue line situated at the lower part represents Coal 2. The black line between the purple zone and pink zone is Coal 3. The dark blue line at the top denotes Coal 4. The top (red wavy line) and bottom (green line) boundaries in this well section are the base of Ketch formation and the top of Caister sandstone, respectively.

Four widely distributed coal seams namely Coal 1, Coal 2 (Durham Low Main coal/ sub-B coal), Coal 3 (Main coal/ B coal), and Coal 4 are identified and correlated (Fig. 5.11) according to their locations and log response (Table 5.5). The lower two Coal seams which are Coal 1 and Coal 2 have a low uranium response which is lower than 3 ppm. But Coal 2 also has a high thorium response, which is different from Coal 1. The URAN of Coal 3 and Coal 4 is higher than 3 ppm.

These coal seams are thicker in the southern area and become thinner in the central area as well as Quadrant E (Fig. 5.11). None of them can be traced in the northern area, especially at the location of Well 44/12a-3. Coal 1 is closed to the Caister Sandstone. Most of it was deposited and preserved in the southern area. Coal 2 is near Coal 3 but usually thinner than Coal 3. Both of them are usually studied together since they can be distinguished even in the other areas. Coal 3 is the thickest coal seam in the whole interval and covers the largest area. The thickness of Coal 3 ranges from 0.8 m to 4.28 m. Coal 4 is the most locally deposited. It can extend to the central area but most of it is found in the southern area. In the vertical direction, Coal 4 is usually located between base W4c and base IG3. And it is relatively thinner compared to the other three coal seams.

Table 5.5 Characteristics of correlated coal seams

Coal seams	Other names	Thickness/m	Location	Log response
Coal 1	+1 coal	0.42~2.03	Near the top of Caister SST	URAN: low (<3 ppm) U/Th: low (<0.5)
Coal 2	Durham Low Main coal/ sub-B coal/ B coal	0.54~3.19	In the middle of W4a/IG1	URAN: low (<3 ppm) U/Th: high (>0.5)
Coal 3	Main coal/ B coal/ C3 coal	0.8~4.28	Between base W4b and base IG2	URAN: high (>3 ppm) U/Th: high (>0.5)
Coal 4	-	0.31~2.76	Between base W4c and base IG3	URAN: high (>3 ppm) U/Th: high (>0.5)

5.5. Correlation of cyclothems

The cyclothems in the lower succession have been correlated in some closely-spaced wells (Fig. 5.12) in this study, aiming at proving a plausible idea for further study about higher-resolution stratigraphy and lateral consistency of facies. The well-defined cyclothems with the visible coarsening-upward trend are easier to connect while the less well-defined cyclothems that are usually thicker and lack coal seams or sandstone are relatively hard to correlate. For well-developed cyclothems correlation, the boundaries are generally the top of the coals. The boundaries separate the lower coal seams and upper floodplain

deposits. While for less well-defined cyclothem correlation, the boundaries are usually the surfaces between the top of sandstone and the bottom of floodplain deposits. When the floodplain deposits are longer than 20 meters without visible change of GR values, the correlation becomes challenging.

Similar sedimentary patterns can indicate the same depositional environment or the different parts of one environment deposited at the same time, which provides a hint to correlate. One possible small-scale framework of lower succession in 44/23 wells (Fig. 5.12) indicates that the lateral extent of one cyclothem can reach 3-15 km. However, the lateral heterogeneity of cyclothem developed in the 44/22 wells which are situated in another area is greater than in the 44/23 wells. The high-resolution cyclothem correlation that is only based on wireline logs is challenging to work.

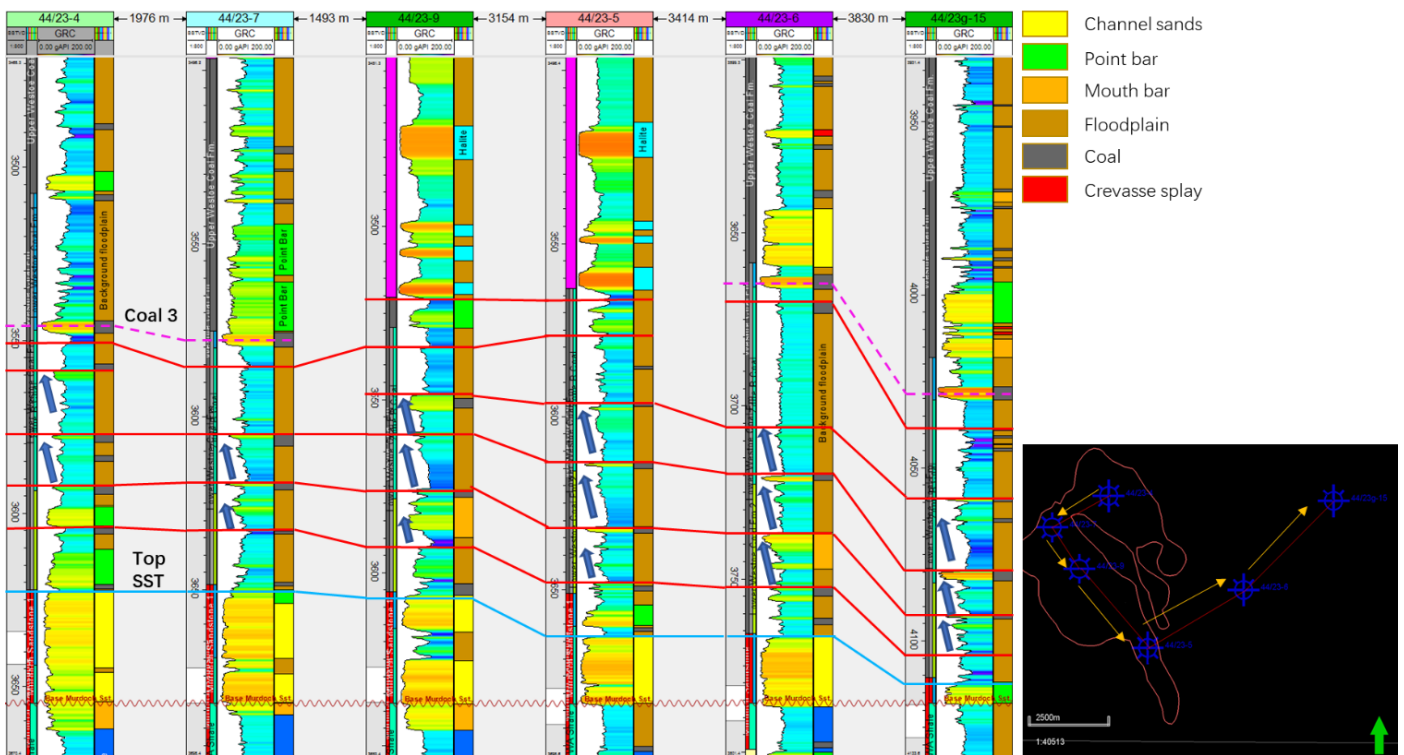


Fig. 5.12 Correlation of cyclothem in the 44/23 wells. The facies interpretation here came from the Wintershall company. Note that the blue line represents the top of Caister SST and the dashed line indicates the Coal 3.

6 Discussion

In this chapter, the limitation and reliability of the results will be discussed at first. It will be analyzed from the accuracy of the data, the limitations of each applied method, and the feasibility of the outcome. Afterwards, an integrated stratigraphic framework referring to the intermediate-scale units will be given and the sedimentary system will be studied based on the consistency of stratigraphy. The relation between cyclothem and small-scale INPEFA cycles will be discussed in order to provide a basis for further higher-resolution correlation. In the end, whether the identified units of two scales are related to astronomical climate forcing will be studied.

6.1. Limitation and reliability of the results

Data had different calibrations and origins and therefore comparison was difficult in some cases. Also, the measurement quality of some wells is not optimal. These lead to the overlaps of wireline log values of different lithofacies (Fig. 5.1) and increasing the difficulty of setting the cutoff values. Thus, the determination of cutoff values may not apply to all wells because of the different measurement scales. Besides, the thresholds of the same logging curve between different lithologies have overlapping parts which cause careful definition of cut-off values. When further dividing the sedimentary facies of sandstone, the selection of coefficients of regression curve may not be accurate, though it follows the logic of manual interpretation. In other words, sedimentary facies such as mouth bars contain fine-grained to coarse-grained sandstone, but the fine-grained part may be determined as non-sandstone during the identification of electrofacies. Hence, it leads the deposits of the same sedimentary facies to be divided into two parts and the fine-grained part to be excluded.

The verification of electrofacies has some limitations because the core coverage of the Westoe Coal and Caister formations is focused on reservoir intervals. Six wells are used to evaluate the electrofacies, and four of them only contain useful core materials or FMI data with a thickness of no more than 50 meters. Some thinner coal seams less than 0.2 m are hard to identify due to the resolution of logging data. In addition, the logging response of different types of coal varies. For instance, the strongly compacted coal seams have a higher density, and the coal seams containing shale have a higher GR value. These distinct coal seams are not recognized during electrofacies interpretation.

Biostratigraphy in the study area principally relies on the pollen recognized from cuttings as well as core samples. The sampling interval ranges from a few meters to around 20 meters, which means the depth of

the boundaries could not be very accurate. Though the boundaries of biozones are exact tie points and a level of error needs to be taken into account, some of the biozones have been tied to major marine bands and have an isochronous indication. Thus, the biostratigraphical framework can serve as a good constrain to the integrated stratigraphy.

INPEFA method can aid in visualizing stratigraphical breaks in unseen wireline log data and allows the construction of a correlation framework at different scales. Applied to facies sensitive log, the identified INPEFA stratigraphic intervals are linked to the vertical variation of lithofacies, which means this method is correlated to the lithostratigraphy in the background. Specifically, the negative trend corresponds to the percentage of sandstone gradually decreases from bottom to top, and the positive trend is in line with net-to-gross ratio increases upwards (Fig. 4.5). The defect of this method itself is that it might be assumed to ignore the influence of tectonics. In this study, the tectonic processes are not taken into account, as the short time-scale lithofacies change is mainly controlled by climate patterns, and the subsidence is thought to be relatively uniform without abrupt structural events during middle Westphalian (McKenzie D, 1978; Schroot B M et al, 2003; Bailey J B et al, 1993). This is also demonstrated in De Jong et al (2007) where they stated that climate-controlled patterns can be regarded as superimposed on tectonic patterns and the short-term tectonic movements are unable to impact the INPEFA correlation.

INPEFA approach was also applied in De Jong et al (2007) and several stratigraphic packages were classified. The results of this study show a good correlation with De Jong et al. (2007), although some packages are inconsistent. The W4000 stratigraphic package in his study comprises IG1 and IG2 in our study. The top boundary is slightly different in the wells in Quadrant E. The W5000 looks to correspond to IG3 and IG4 identified in this study, and IG5 and IG6 are included in the W6000. However, his work only focused on INPEFA interval without considering other stratigraphic methods. This results in different conclusions of the stratigraphic packages. De Jong argues that the middle W5000 is laterally impersistent due to erosion. However, others observe no severe erosion or interruption of sedimentation during the deposition of the Westoe Coal formation (O'Mara, 1999; Richard et al., 2020). After comparison with the biozones, it seems reasonable that the top IG5 and IG6, corresponding to W5b and W6a biozones, did not develop in the northern area or relatively thin deposits in the northern area were eroded by the top Ketch sandstone formation which deposited during active tectonic events.

Unlike Caister sandstone deposited in the high systems tract to low systems tract stage, the deposition of fluvial sand-bodies in the transgressive systems tract is relatively local (Collinson et al., 2005), increasing the difficulty of correlating sandstone on the regional scale. Moreover, the sandstone connection in the whole area is low due to the fast deposition rate and the impact of autogenetic processes. Therefore, the correlation of coal seams and the study of isochronism of lithofacies that link to cyclothems is valuable.

Thin, less frequent coals with thick alternation of sandstone and floodplain deposits appear in the upper interval and thick, more frequent coals with fewer sandy deposits show in the lower succession. This feature

was also observed by O'Mara (1999). He thought it was the result of the culmination of the increasing rate of stratigraphic base-level rise in the late Westphalian B. During the development of the 3rd order transgressive systems tract, peat swamps rapidly drowned and lakes formed as a result of the quick base-level rise. Meanwhile, marine incursions became apparent, and MB's show an increased abundance, indicating large accommodation space where a large amount of sandstone can deposit. Basinal topography was thought another influential factor superimposed on the stratigraphic base-level rise in the late Westphalian B since the Variscan foreland basin was closing responding to the northward migration of the Variscan front (Leeder and Hardman, 1990; O'Mara, 1999). This led the palaeoslope to become steeper concomitant with the rise of base-level, more sandy input, and less coal formation. These explanations are well-founded and in line with the observation and correlation developed in this study. Therefore, the regional-scale coal seams correlation in the lower part of the interval is relatively reliable, and its geographic extent can be closed to the dimensions of the lake coals filled which can reach 15 km in width.

Comparing the stratigraphic packages and biozones, the position of boundaries of the two zones/packages is not completely consistent and the thickness trends differ in some wells. The possible reason is that the man-made division of biozones and INPEFA stratigraphic packages are not precise. Besides, the 2D maps made by convergent interpolation have some uncertainties because only the wells containing the data of biozones are used to calculate. They can be used to study the trend of the thickness of each stratigraphic zone. However, limited data is used to calculate and the maps are predicted by mathematical methods, so the thickness of the location where there is no available well data may not be very accurate. The main coal seams that are widely distributed in the study area could assist generate a smaller-scale correlation. The coal seams correlation could decrease the variation between the biozones and INPEFA stratigraphy. For instance, Coal 4 deposited between base W4c/d and base IG3.

6.2. Integrated stratigraphy

There is a good correspondence between INPEFA stratigraphic packages and biozones because the depth offset of boundaries between two zonations is small (Fig. 2.1, Appendix E). The thickening trends of most zones towards the southwest could indicate that the southwest area is the center of the depo-basin. It is in line with the palaeotopography (Fig. 2.2). The southwest part of the study area is in the Silver Pit basin and the northeast area is closed to the Cleaver High and North Sea High areas. The Westoe Coal formation and Cleaver formation are thought to be deposited during the transgressive systems tract (O'Mara, 1995; Quirk, 1997; Schrijver et al, 2020). And the sea level increased during the deposition of these two formations. The accommodation space is where sediments can be deposited and it is controlled by the sea level and structure. Therefore, the accommodation space could be the reason causing the variation of deposition in northern and southern areas.

For both biostratigraphy and INPEFA stratigraphic packages, the middle two zones are missed in the northern area and the top two zones are only traced in the southern area. The possibility is that they didn't deposit, or only little sediments were deposited and were removed by upper sands in the northern area where accommodation space is smaller compared to the southern area. The reason is that no strong structural events happened during the deposition of the Westoe Coal formation (McKenzie D, 1978; Schroot B M et al, 2003; Bailey J B et al, 1993), which means that no severe erosion occurred. The sands deposited by braided channel in Westphalian B is thought to be unable to remove many sediments (O'Mara, 1995). The removed part could be approximately one cyclothem less than 15 m at the bottom (O'Mara, 1995). In addition, the top defined two zones usually refer to the Cleaver formation. The provenance of Cleaver formation was thought to lay to the south (Collison, 2005). Thus, it is plausible that the sediments from the south were deposited in the Silver Pit basin and not many could reach the higher northern area.

6.3. Cyclothem and short-term INPEFA cycles

Four types of cyclothem including well-defined and less well-defined types are identified (Fig. 6.1). The lithology combination of well-developed cyclothem that are type 1 is closer to the rock types of ideal cyclothem. They consist of fine grains, sands, and coals seams from bottom to top with a visible coarsening-upward trend. The less well-defined cyclothem usually lack some rock records and the shape of GR is different from the ideal cyclothem's. Many less well-defined cyclothem lack coarse-grained sands, and some of them lack coal seams at the top, which increases the difficulty of accurately recognition and comparison with astronomical cycles. Nonetheless, these distinguishing features can serve as the basis for the high-resolution cyclothem correlation because they are strongly related to the sedimentary patterns and have the capability of reflecting the lateral change of the environment.

Compared to the lithofacies and electrofacies, small cycles of the INPEFA curve correspond to both well-defined and less well-defined coarsening-upward cyclothem in most cases. They could also correspond to thick lacustrine shale columns or thick sandstone successions with some interval GR change (Fig. 5.9). In line with the features of cycles, less well-defined cyclothem occur more often in the places where average cycles are relatively thin and vice versa. Simultaneously, the range of the calculated thickness as well as the difference between INPEFA and visual cyclothem identification based on GR logs is larger in these wells (Fig. 5.10).

Furthermore, short-term INPEFA is applied to the potassium log, and the potassium log is strongly related to the clay content. The clay minerals depend on the source rock. Hence, the short-term INPEFA cycles can reveal the rhythm of clay content that is related to the source. The patterns displayed by short-term INPEFA cycles are different from the GR (Fig. 5.9), and also link to the intermediate-scale zonations. Constrained by

biozones and INPEFA stratigraphic packages, cycles identified by short-term INPEFA of POTA have the potential to effectively assist the small-scale correlation. Further research can pay more attention to this approach and smaller scale.

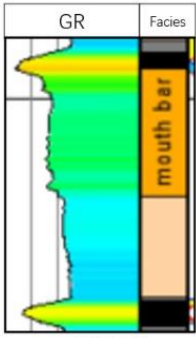
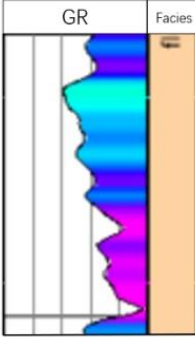
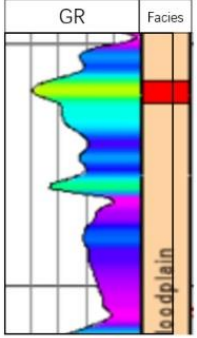
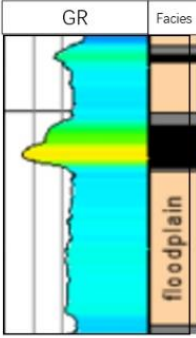
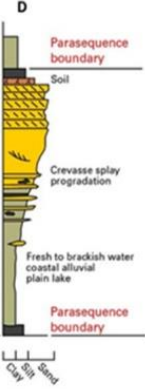
Type	Type 1	Type 2	Type 3	Type 4	Ideal type
Template	 <p>(44/28-2)</p>	 <p>(E17-A2)</p>	 <p>(E17-A2)</p>	 <p>(44/28-2)</p>	 <p>D</p> <p>Parasequence boundary</p> <p>Soil</p> <p>Crevasse splay progradation</p> <p>Fresh to brackish water coastal alluvial plain lake</p> <p>Parasequence boundary</p> <p>Scale: 0, 10, 20, 30, 40, 50, 60, 70, 80, 90, 100</p>
Characters	Coarsening-upward; floodplain deposits at the bottom; sandy deposits in the middle; coal and soil at the top.	Coarsening-upward; floodplain deposits at the bottom; lack of coarse-grain sands; lack of coal.	Coarsening-upward; floodplain deposits at the bottom; sandy deposits in the middle; lack of coal.	No obvious trend; lack of coarse-grain sands.	Ideal cyclothem: coarsening-upward; floodplain deposits at the bottom; sandy deposits in the middle; coal and soil at the top. (after Tucker et al., 2003)

Fig. 6.1 Summary of different types of cyclothem developed in the study area and their characteristics.

6.4. Astronomical forcing and climate-controlled cycles

Two order cycles were identified in the integrated stratigraphy developed in this study. The intermediate-scale zonations comprise biozones and INPEFA stratigraphic packages. Also, the marine bands and coal seams are included in the correlation. Biozones and coal seams are widely accepted as near-synchronous well-to-well correlations. INPEFA curves enable showing the waveform properties of the data and are widely regarded as a further step developing as a method for studying global cyclostratigraphy (Perlmutter et al., 1990). The reason is that the cyclic depositional patterns that are assumed to be formed by tectonic, climate processes and driven by orbital forcing can be predictive (De Jong et al., 2007). To be more specific, the climate change that is orbitally forced by the Milankovitch model can be reflected by vertical lithofacies successions which can be detected using the INPEFA stratigraphic packages (Perlmutter et al., 1990).

However, in our study the thickness variation of medium-term stratigraphic packages is large. The difference inside one stratigraphic package can reach more than 70 m and the standard deviation can be up

to 42 m. It indicates that the intermediate-scale zones could be near-synchronous. The variable thickness does not suggest they are astronomical-controlled cycles. The possible reason could be variations in palaeoslope, sedimentation rates, and tectonic movements in different areas that play significant roles during deposition.

In order to confirm this idea, the INPEFA method is also applied to Well KPK-01, which was used to study the astronomical cyclicity of Upper Carboniferous in Bosch's thesis (2008). The orbital cycles of short eccentricity were thought to be 54 m. The obliquity cycles were around 20 m, and the precessions cycles were about 11 m (Bosch, 2008). The Aegiranum MB and Malby MB were recognized (Bosch, 2008) and they are close to the strongly negative turning points in both medium and short-term INPEFA. Three stratigraphic packages are identified between the Aegiranum MB and the Malby MB in this well (Fig. 6.2). However, the variable thickness does not correspond to any astronomical cycles described in the thesis.

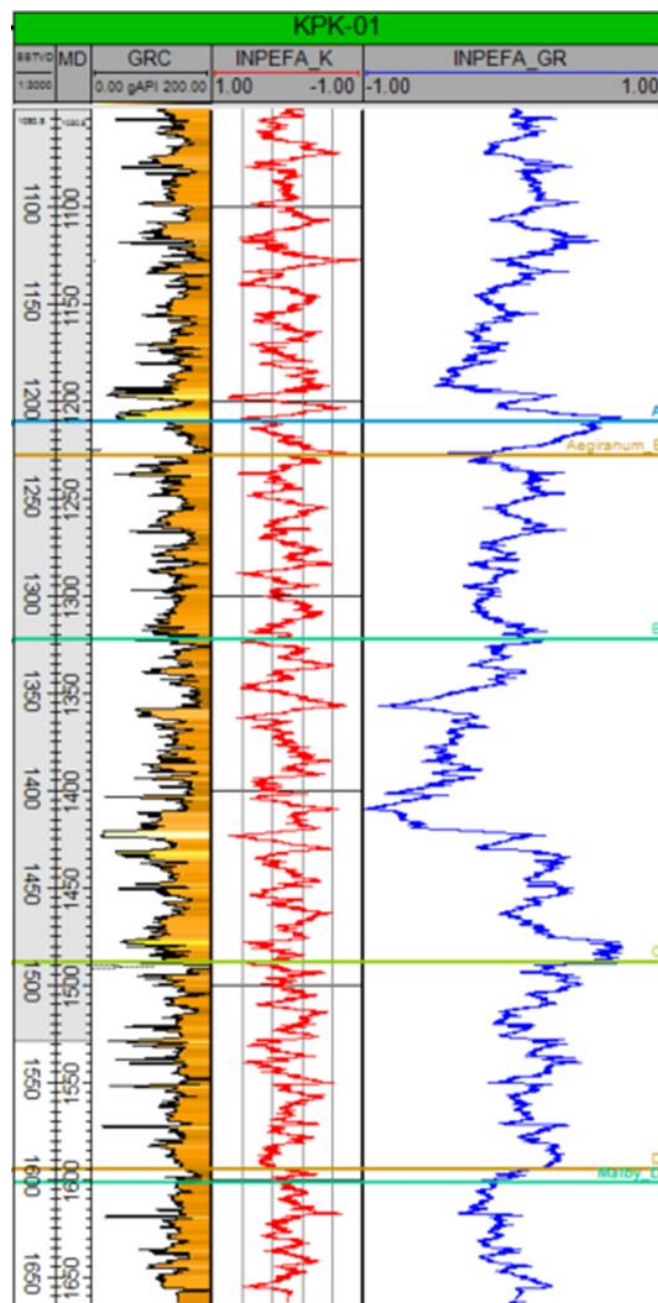


Fig. 6.2 Result of INPEFA with the divided stratigraphic packages and MBs in Well KPK-01. The first column is true vertical depth. The second column represents measured depth. The third column is the GR log, and the fourth column is the short-term INPEFA of POTA. The last column indicates the medium-term INPEFA of GR.

The cyclothem and short-term INPEFA cycles also vary in thickness but within expected heterogeneous character. The small-scale cycles formed in the northern area are usually thinner, more or less 10-12 m, while the thickness of cyclothem in the southern part is approximately 11-13 m. It could indicate that the astronomical cyclicity in the cyclothem scale was better recorded by petrophysical data than the longer-period cyclicity, and it has the potential to be extracted.

Cyclothem and astronomical force in the same interval developing in Europe have been studied for a long time but the duration is various in different papers (Table. 6.1). The global time scale of Westphalian B is 2.5 Myr according to Regional Stratigraphic Reference Scales of East Europe, Central and West Europe, Tethys, South China (eastern Tethys), and North America (Menning et al., 2006). Bosch (2008) applied spectral analysis methods to wireline logs to calculate the duration of cycles deposited in Westphalian B of onshore Dutch. The coal-shale alternations identified in Bosch's master thesis (2008) are linked to climatic precession whose duration time is about 19 kyr. The duration of Westphalian B calculated by the identified cyclicity and the number of cycles is approximately 1.1 Myr (Bosch's, 2008). Van Den Belt et al (2002) used U/Pb radiometric ages to obtain the duration of eccentricity cycles and different stages of Westphalian in the Netherlands. The average cyclothem thickness in Van Den Belt et al (2012) measured at 12.5 m, which equals 21 kyr based on a linear thickness-timespan relation with eccentricity cycles. Van Den Belt et al (2012) suggested that there is no specific control by precession or obliquity due to the variable thickness of individual cyclothem, but pointed at cycle interference.

Table. 6.1 The duration of the stage Westphalian B and some astronomical periods and their corresponding thickness, from Menning et al (2006), Bosch (2008), and Van Den Belt (2012).

Stage	Duration, Menning et al. (2006)	Duration, Bosch (2008)	Thickness, Bosch (2008)	Duration, Van Den Belt et al. (2012)	Thickness, Van Den Belt et al. (2012)
Westphalian B	2.5 Myr	1.1 Myr	-	1.2 Myr	-
Precession	-	19 kyr	11 - 18 m	17 kyr	-
Obliquity	-	34.2 kyr	~20 m	35 kyr	-
Short-eccentricity	-	100 kyr	~54 m	93 kyr	~60 m
Cyclothem	-	19 kyr	11 - 18 m	21 kyr	~12.5 m

The Well 49/2-3, 49/1-3, and 44/27-1 contain the most cyclothem and relatively complete Westphalian B formation in the study area. There are about 33 cyclothem measured in Westphalian B, with an average thickness of about 12 m. Approximate 34 cycles were identified by short-term INPEFA in the same interval with an average thickness of nearly 11.8 m. The timescale of the Westphalian B calculated by the number of cycles and obliquity period in the study area is equal to $34 \times 34.2 = 1.16$ Myr or $34 \times 35 = 1.19$ Myr. It is closed to the duration of Van Den Belt (2012) and Bosch (2008). What needs to be noted is that the number of cyclothem in the computation is different from the total number of cycles in the study interval. The study interval contains Westphalian B and lower Westphalian C stages and thus, the number of cycles is larger. The counted duration of Westphalian B could not be the absolute duration of the time interval because the cycles could not be detected or some cycles were eroded after deposition. The effect of the falling systems tract and the duration of Caister sandstone are not taken into account during calculation, which can also influence the accuracy of the calculation.

Nevertheless, the cyclothem in the study area are largely affected by the obliquity force based on the computed results. But the interference of different cycles such as high-amplitude precession causing splitting of longer-period obliquity cycles reflected by various thicknesses could also exist. Compared to the cyclothem deposited in the onshore Netherlands, the cyclothem in the study area are thinner, and the influence from obliquity looks stronger. The most likely number of INPEFA cycles is 32 and the computed average thickness is equal to 11.67 m in Well KPK-01 (Fig. 6.2), which is close to the length of precession cycles (Bosch, 2008). The difference in controlling astronomical forcing could be caused by different sedimentary systems and Palaeotopography. The onshore Netherlands is situated on the south bank, opposite the research area in this study. The accommodation space and the sedimentary velocity could be different. Compared with the northern source in the study area, the southerly provenance of onshore Netherlands contained fewer sands and thus no typical cyclothem are observed. The cyclicity in the onshore Netherlands consists of floodplain deposits and coal seams, showing different log responses. Additionally, the long-period, 100 & 400 kyr eccentricity forcing studied in Bosch (2008) is not found in this study.

7 Conclusion

In this study, an intermediate-scale integrated stratigraphic framework (Appendix G) with a vertical resolution of tens of meters to around 150 meters has been constructed by using integrated methods including biostratigraphy, INPEFA stratigraphy, and lithostratigraphy. The boundaries of the biozones and INPEFA stratigraphic packages are not exactly the same, but the two approaches match each other. The offset of the two types of zonation is usually 2-15 m. Four major coal seams that cover most of the study area are correlated, which could assist further smaller-scale stratigraphy. Sandstone correlation is hard to be applied on the regional scale and the recognition of marine bands is not ideal in some wells. Thus, such correlations of them are not included in this study.

The lateral extent of the lower intermediate-scale zones which are W4a/IG1 and W4b/IG2 is wide, covering nearly the whole study area. From bottom to top, the coverage of the zones becomes smaller. The top zones W5b/IG 5 and W6a/IG6 only appear in the southern area. The thickness of each zone varies. The biozones generally show a trend that is thinner in the northern area and becomes thicker southward, while such a feature is not that obvious in the stratigraphic packages where the thickest zone is found in the middle area. Possible reasons are discussed as the inherent uncertainties of the two stratigraphic methods, the influence of paleomorphology, the difference in sedimentation rates, and the subsequent tectonic effects in late Westphalian B.

Thick coal seams are more frequent in the lower succession and more sandy deposits are found in the top of the succession. The most significant coal seam which is Coal 3 can cover the most study area despite some absence in the middle. Large-scale coal seams are thought to be related to large-scale flooding events like marine incursions that can quickly swamp the whole region and formed the environment of the lake. Other widely spaced coal seams can reach 15 km wide which could be the dimension of a lake where coal seams filling in.

The small-scale cyclicity consisting of cyclothems which range from 7 to 15 m in the study area can be identified and extracted by short-term INPEFA or POTA. Most well-defined cyclothems are coarsening upward, comprising floodplain deposits, sand-bodies, and coal seams at the top. There are also some less well-defined cyclothems with different sediments input, but the sedimentary patterns are similar. The lateral extent of small cyclothems varies in different locations and at different intervals. The correlation of small cyclothems can be achieved in closely spaced wells where the distance is no longer than 4 km. More detailed lateral facies variations and small-scale correlation can be further studied based on the small-scale INPEFA cycles.

The integrated stratigraphy could be regarded as near-synchronous correlations. No longer-period astronomical cycles are recognized due to the highly variable thickness related to the detected units. And the thickness variation of each intermediate-scale zone classified in this study is large. During the deposition of intermediate-scale units, the sedimentation rate, palaeoslope, and later tectonic events could play an important role. The small-scale cyclothems could be controlled by the obliquity force considering the average thickness which is equal to 12 m and the calculated duration of Westphalian B. The duration of obliquity cycles is nearly 35 kyr and the calculated time span of Westphalian B in the study area is close to 1.2 Myr.

Bibliography

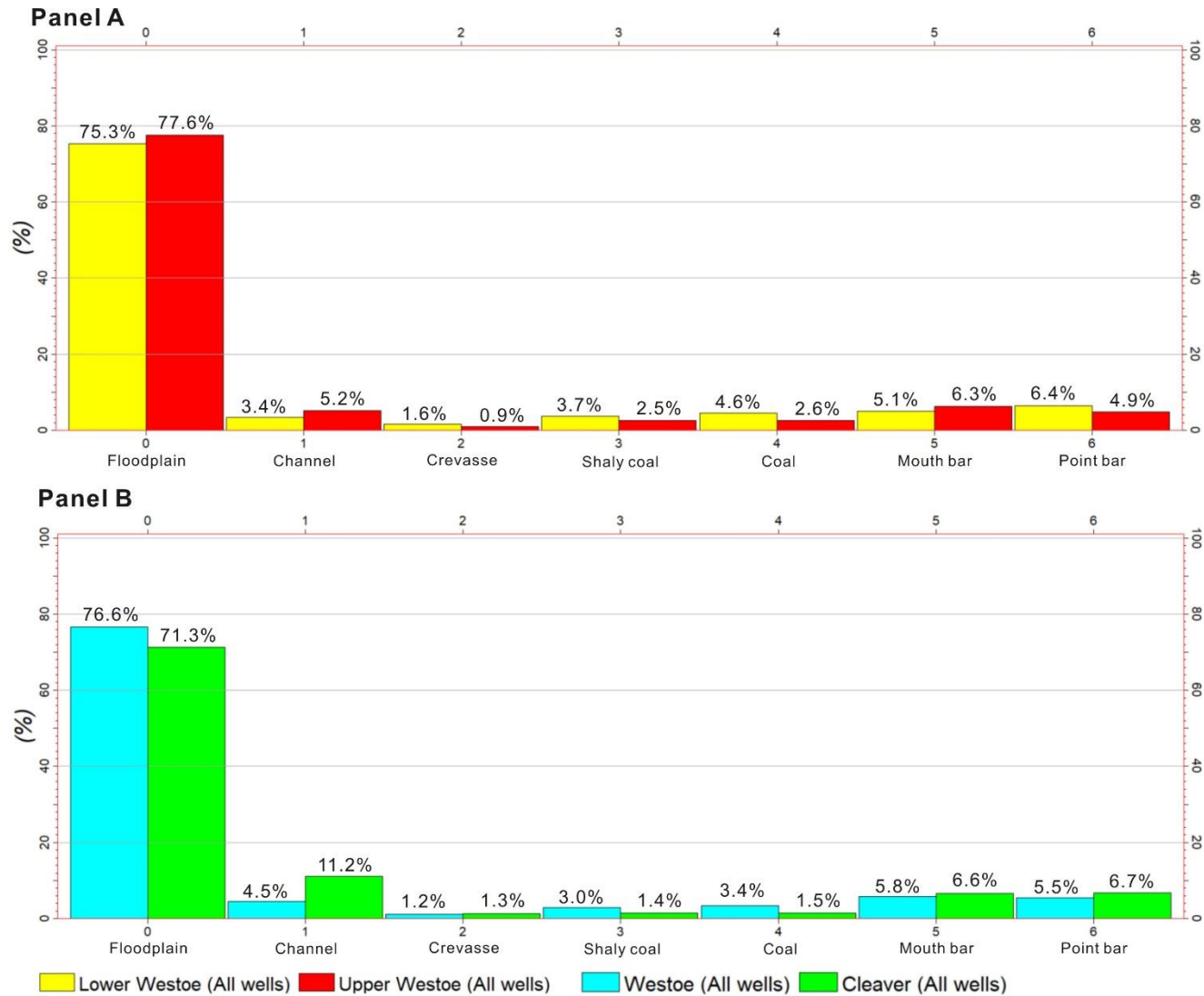
- [1] Bailey J B, Arbin P, Daffinoti O, et al. Permo-Carboniferous plays of the Silver Pit Basin[C]//Geological Society, London, Petroleum Geology Conference Series. Geological Society of London, 1993, 4(1): 707-715.
- [2] Besly, B.M. 1990. Carboniferous. In: Glennie, K. W. (ed.) Introduction to the petroleum geology of the North Sea. Blackwell Scientific Publications, Oxford. 3rd edition, 90-119.
- [3] BESLY, B. M. 1998. Carboniferous. In: GLENNIE, K. W. (ed.) Petroleum Geology of the North Sea: Basic Concepts and Recent Advances (fourth edition). Blackwell Science, Oxford, 104-136.
- [4] Besly, B. M. 2002. Late Carboniferous redbeds of the UK southern North Sea viewed in a regional context [abstract: pp. 17–19]. Paper presented at “Hydrocarbon resources of the Carboniferous, southern North Sea and surrounding onshore areas” conference, Yorkshire Geological Society, Sheffield, 2002. This volume: 225–226.
- [5] Binzhong Zhou, Graham O’Brien. 2015. Coal quality from geophysical logs for enhanced resource estimation. Final report for ACARP Project C23015. COAL MINING PROGRAM/ENERGY.CSIRO Energy Report: EP157964.
- [6] Bos A. D., Alternative interpretation of maximum entropy spectral analysis. IEEE Transactions on Information Theory, 1971, 17(4): 493-494.
- [7] Burg J. P., Maximum entropy spectral analysis. Proceedings of 37th Annual International Meeting, Society of Exploration Geophysics, Oklahoma City, USA, 1967.
- [8] B.Pradier, G.Nicolas. 1995. The Netherlands Extensive Offshore E/16-3. Petrographic analysis of coal seams from core N°3. Elf Aquitaine Production. EP/P/EXP/TIS n 95.5.5 RP/GO.
- [9] C.M. Henderson, S.Z. Shen, F.M. Gradstein, F.P. Agterberg. Chapter 24 - The Permian Period. Geologic Time Scale 2020. Elsevier, 2020, Pages 875-902.
- [10] Cameron, T. D. J. 1993b. Carboniferous and Devonian of the southern North Sea. In Lithostratigraphic nomenclature of the UK North Sea (vol. 5), R. W. O’B. Knox & W. G. Cordey (eds), 1–93. Nottingham, British Geological Survey.
- [11] Cameron N, Ziegler T. Probing the lower limits of a fairway: further pre-Permian potential in the southern North Sea[J]. Geological Society, London, Special Publications, 1997, 123(1): 123-141.
- [12] Carboniferous (Westphalian) of the Anglo-Dutch Basin using the climate stratigraphic approach, ENRES Technical Paper Series, 2007.
- [13] Cecil C B. The concept of autocyclic and allocyclic controls on sedimentation and stratigraphy, emphasizing the climatic variable[J]. 2003.
- [14] Collinson, J.D., Jones, C.M., Blackbourn, G.A., Besly, B.M., Archard, G.M. & McMahon, A. 1993. Carboniferous depositional systems of the Southern North Sea. In: Parker, J.R. (ed.), Petroleum Geology of Northwest Europe: Proceedings of the 4th Conference. Geological Society of London. 677-687.
- [15] De Jong M G G, S.D. Nio, D. Smith, and A.R. Böhm, 2007. Subsurface correlation in the Upper Carboniferous (Westphalian) of the Anglo-Dutch Basin using the climate stratigraphic approach. First Break 25, no 12. December 2007, pp. 49-59.
- [16] De Jong M G G, Donselaar M E, Boerboom H T W, et al. Long-range, high-resolution stratigraphic correlation of Rotliegend fluvial-fan deposits in the central Dutch offshore[J]. Marine and Petroleum Geology, 2020, 119: 104482.

- [17] Don Cameron, Jim Munns, Sue Stoker. Remaining hydrocarbon exploration potential of the Carboniferous fairway, UK southern North Sea. ages 209–224 of Carboniferous hydrocarbon geology: the southern North Sea and surrounding onshore areas. Published as volume 7 in the Occasional Publications series of the Yorkshire Geological Society, © Yorkshire Geological Society 2005.
- [18] ENRES stratigraphic methods and workflow approaches in subsurface well correlations. THE INPEFA LOG TRANSFORM AND STRATIGRAPHIC INTERPRETATION MODELS. Open file report. Report ID: ES484-2011/Version October 2011. <https://cyclog.com/wp-content/uploads/2014/09/ENRES-Stratigraphic-methods-and-workflow-approaches-in-subsurface-well-correlations-compressed.pdf>
- [19] F.J.G. van den Belt et al. Sedimentary cycles in coal and evaporite basins and the reconstruction of Palaeozoic climate. Utrecht Studies in Earth Sciences.
- [20] Fisher Q J, Wignall P B. Palaeoenvironmental controls on the uranium distribution in an Upper Carboniferous black shale (*Gastrioceras listeri* Marine Band) and associated strata; England[J]. *Chemical Geology*, 2001, 175(3-4): 605-621.
- [21] Gradstein, F.M., Ogg, J.G., and Smith, A.G., 2004, A Geologic time scale 2004, Cambridge University Press, 589 p. Hampson, G., Stollhofen, H., and Flint, S.,
- [22] Hiroshi Yamada and Gawon Yoon. 2015. Selecting the tuning parameter of the ℓ_1 trend filter. *Studies in Nonlinear Dynamics & Econometrics*. DOI: 10.1515/snde-2014-0089
- [23] J. D. Collinson, D. J. Evans, D. W. Holliday, N. S. Jones. Pages 135–146 of Carboniferous hydrocarbon geology: the southern North Sea and surrounding onshore areas. Published as volume 7 in the Occasional Publications series of the Yorkshire Geological Society, © Yorkshire Geological Society 2005.
- [24] Jirásek J, Opluštil S, Sivek M, et al. Astronomical forcing of Carboniferous paralic sedimentary cycles in the Upper Silesian Basin, Czech Republic (Serpukhovian, latest Mississippian): New radiometric ages afford an astronomical age model for European biozonations and substages[J]. *Earth-Science Reviews*, 2018, 177: 715-741.
- [25] Kendall C . 2003. Use of well logs for sequence stratigraphic interpretation of the subsurface. USC Sequence Stratigraphy Web. University of South Carolina.
- [26] Kim, S., K. Koh, S. Boyd, and D. Gorinevsky, 2009, ℓ_1 trend filtering, *SIAM Review*, 51,2, 339–360.
- [27] Kombrink H. The Carboniferous of the Netherlands and surrounding areas; a basin analysis. *Geologica Ultraiectina* (294)[M]. Departement Aardwetenschappen, 2008.
- [28] Leeder, M.R., Hardman, M., 1990. Carboniferous geology of the southern North Sea Basin and controls on hydrocarbon prospectivity. In: Hardman, R.F.P., Brookes, J. Eds., *Tectonic Events Responsible for Britains Oil and Gas Reserves*, Vol. 55. Geol. Soc. Lond. Spec. Publ., pp. 87–105.
- [29] McKenzie D. Some remarks on the development of sedimentary basins[J]. *Earth and Planetary science letters*, 1978, 40(1): 25-32.
- [30] McLean D, Murray I. Subsurface correlation of Carboniferous coal seams and inter-seam sediments using palynology: application to exploration for coalbed methane[J]. Geological Society, London, Special Publications, 1996, 109(1): 315-324.
- [31] McLean D, Owens B, Neves R. Carboniferous miospore biostratigraphy of the North Sea[J]. Occasional Publication series of the Yorkshire Geological Society, 2005, 7: 13-24.
- [32] Menning, M., Alekseev, A.S., Chuvashov, B.I., Davydov, V.I., Devuyt, F.X., Forke, H.C., Grunt, T.A., Hance, L., Heckel, P.H., Izokh, N.G., Jin, Y.G., Jones, P.J., Kotlyar, G.V., Kozur, H.W., Nemyrovskaya, T.I., Schneider, J.W., Wang, X.D., Weddige, K., Weyer, D., and Work, D.M., 2006, Global time scale and regional stratigraphic

- reference scales of Central and West Europe, East Europe, Tethys, South China, and North America as used in the Devonian-Carboniferous-Permian Correlation Chart 2003 (DCP 2003): *Palaeogeography Palaeoclimatology Palaeoecology*, v. 240, p. 318-372.
- [33] Noorbergen L J, Abels H A, Hilgen F J, et al. Conceptual models for short-eccentricity-scale climate control on peat formation in a lower Palaeocene fluvial system, north-eastern Montana (USA)[J]. *Sedimentology*, 2018, 65(3): 775-808.
- [34] O'Mara P T, Turner B R. Westphalian B marine bands and their subsurface recognition using gamma-ray spectrometry[J]. *Proceedings of the Yorkshire Geological Society*, 1997, 51(4): 307-316.
- [35] O'Mara P T. Correlation, facies distribution and sequence stratigraphic analysis of the Westphalian B Coal Measures in Quadrant 44 of the southern North Sea[D]. Durham University, 1995.
- [36] O'Mara P, Turner B R. Sequence stratigraphy of coastal alluvial plain Westphalian B Coal Measures in Northumberland and the southern North Sea[J]. *International Journal of Coal Geology*, 1999, 42(1): 33-62.
- [37] Perlmutter, M.A. and Matthews, M.D. [1990] Global cyclostratigraphy – a model. In Cross, T. (Ed.) *Quantitative Dynamic Stratigraphy*, Prentice Hall, 233-260.
- [38] Quirk D G. Interpreting the Upper Carboniferous of the Dutch Cleaver Bank High[C]//Geological Society, London, Petroleum Geology Conference series. Geological Society of London, 1993, 4(1): 697-706.
- [39] Quirk D G. Sequence stratigraphy of the Westphalian in the northern part of the Southern North Sea[J]. Geological Society, London, Special Publications, 1997, 123(1): 153-168.
- [40] Richard Hui In't Veld, Bart Schrijver & Alexander Salzwedel. 2020. The Wingate Field, Blocks 44/23b, 44/24b and 44/19f, UK North Sea. Geological Society, London, *Memoirs*, 52, 1–16, <https://doi.org/10.1144/M52-2018-75>
- [41] Ritchie, J., Pratsides, P., 1993. The Caister Field, Block 44r23a, UK North Sea. In: Parker, R.J. Ed. *Petroleum Geology of Northwest Europe*. Proceedings of 4th Conference, Geol. Soc. Lond. pp. 759–769.
- [42] S.Dijn Nio, Jan Brouwer, David Smith, Mat de Jong, and Alain Böhm. Spectral trend attribute analysis: applications in the stratigraphic analysis of wireline logs. *First Break* volume 23. April 2005, pp. 71-75.
- [43] S.Dijn Nio. *Climate Stratigraphy – A New Approach in Near-Synchronous Subsurface Correlation*. European Association of Geoscientists & Engineers. Jan 2008, cp-258-00018.
- [44] Schrijver B, Salzwedel A. The Wingate Field, Blocks 44/23b, 44/24b and 44/19f, UK North Sea[J]. Geological Society, London, *Memoirs*, 2020, 52(1): 288-303.
- [45] Schroot B M, De Haan H B. An improved regional structural model of the Upper Carboniferous of the Cleaver Bank High based on 3D seismic interpretation[J]. Geological Society, London, Special Publications, 2003, 212(1): 23-37.
- [46] Stewart S A, Coward M P. Synthesis of salt tectonics in the southern North Sea, UK[J]. *Marine and Petroleum Geology*, 1995, 12(5): 457-475.
- [47] Stone P, Millward D, Young B, et al. *Northern England*[M]. British Geological Survey, 2010.
- [48] Tucker M, Gallagher J, Lemon K, et al. The Yoredale cycles of Northumbria: High-frequency clastic-carbonate sequences of the Mid-Carboniferous icehouse world[J]. *Northumbria Rocks*, 2003, 18(26).
- [49] V Cotti Ferrero, *Celestina* (2004-01-01). *Encyclopedia of Sediments and Sedimentary Rocks*. Springer. ISBN 978-1-4020-0872-6.
- [50] W.B.L. Bosch. *Astronomical cyclicity in Upper Carboniferous (Westphalian) fluvio-deltaic sediments in the subsurface of the Netherlands*. Utrecht University MSc thesis, 2008

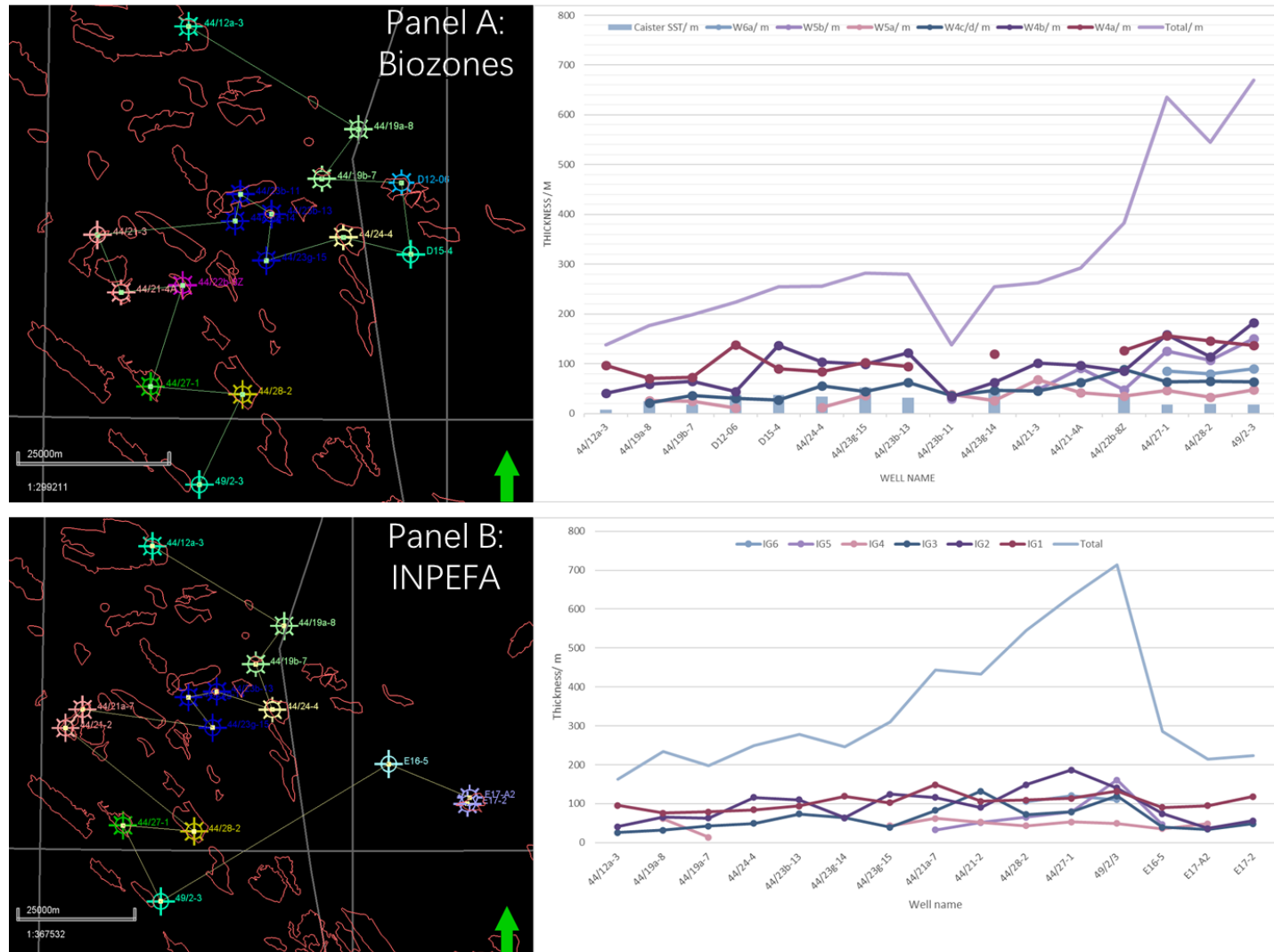
- [51] Weedon G P, Read W A. Orbital-climatic forcing of Namurian cyclic sedimentation from spectral analysis of the Limestone Coal Formation, Central Scotland[J]. Geological Society, London, Special Publications, 1995, 85(1): 51-66.
- [52] Weller, J.M., 1930, Cyclic sedimentation of the Pennsylvanian Period and its significance: Journal of Geology, v. 38, p. 97-135.
- [53] Wilkinson B H, Merrill G K, Kivett S J. Stratal order in Pennsylvanian cyclothems[J]. Geological Society of America Bulletin, 2003, 115(9): 1068-1087.
- [54] Yong H, Juan X, Wenxiang H, et al. Application of high frequency lake level change in the prediction of tight sandstone thin reservoir by sedimentary simulation[J]. Marine and Petroleum Geology, 2021: 105049.
- [55] Zhou B, O'Brien G. Improving coal quality estimation through multiple geophysical log analysis[J]. International Journal of Coal Geology, 2016, 167: 75-92.
- [56] Zhou F, Fredericks L, Luft J, et al. A case study of mapping igneous sill distribution in coal measures using borehole and 3D seismic data[J]. International Journal of Coal Geology, 2020, 227: 103531.

Appendix A. Histogram of the percentage of different electrofacies in different stages.



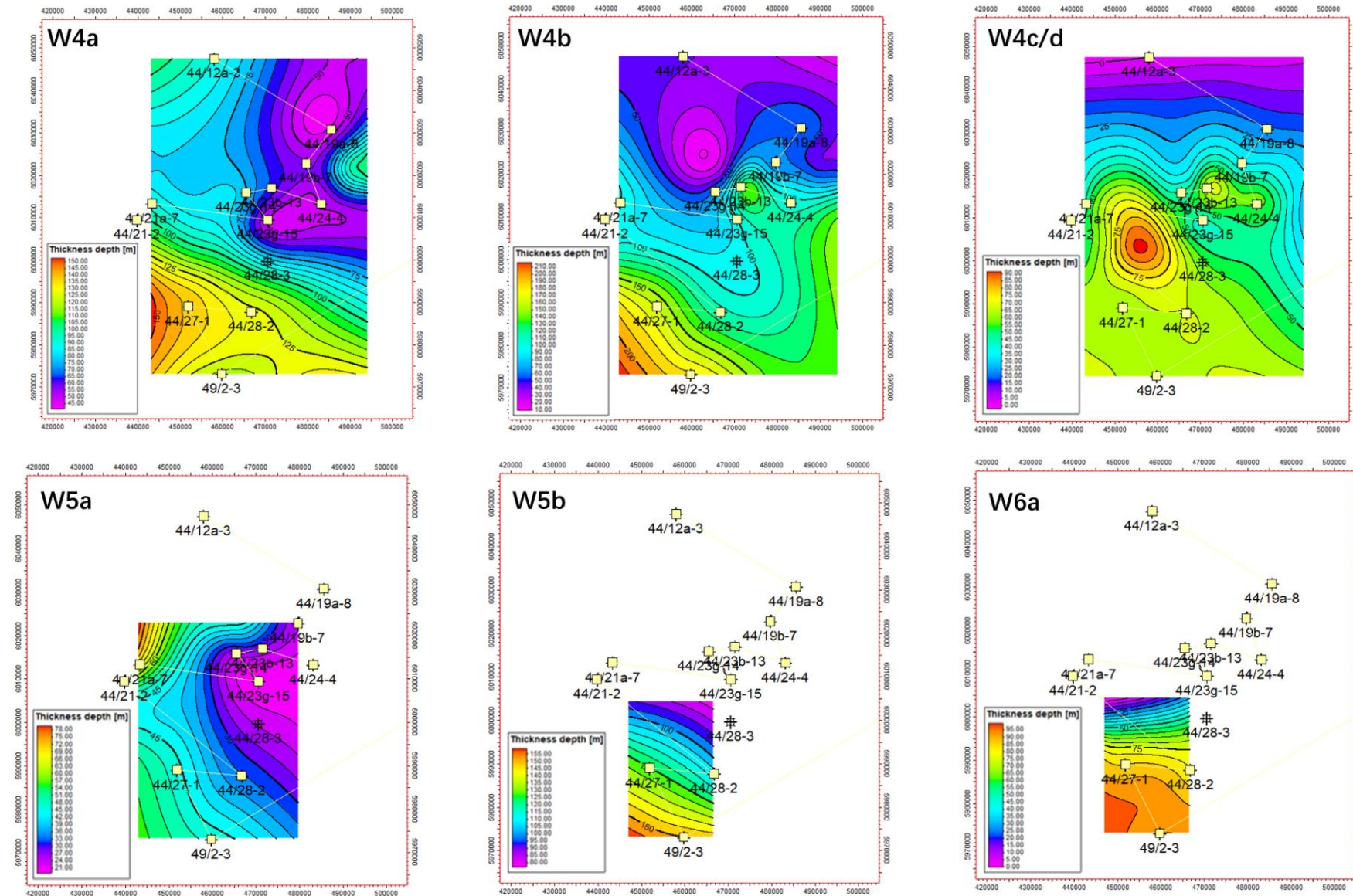
Panel A: The comparison of the percentage of eletrofacies between Lower Westoe Coal formation and upper Westoe Coal formation. Panel B: The comparison of the percentage of eletrofacies between Westoe Coal formation and Cleaver formation.

Appendix B. Thickness distribution of Biozones and INPEFA stratigraphic packages.

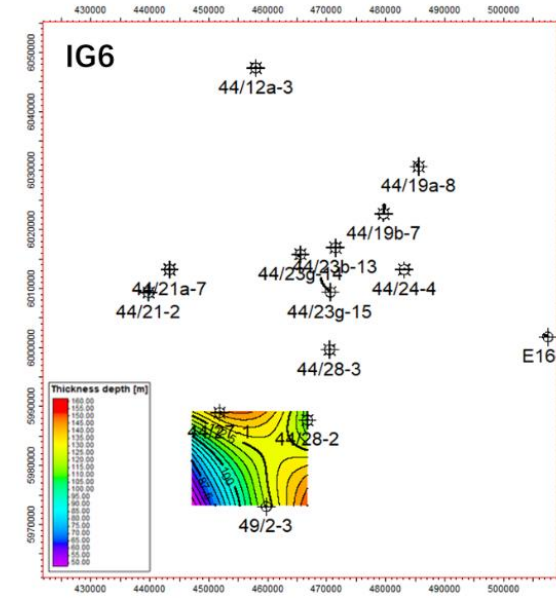
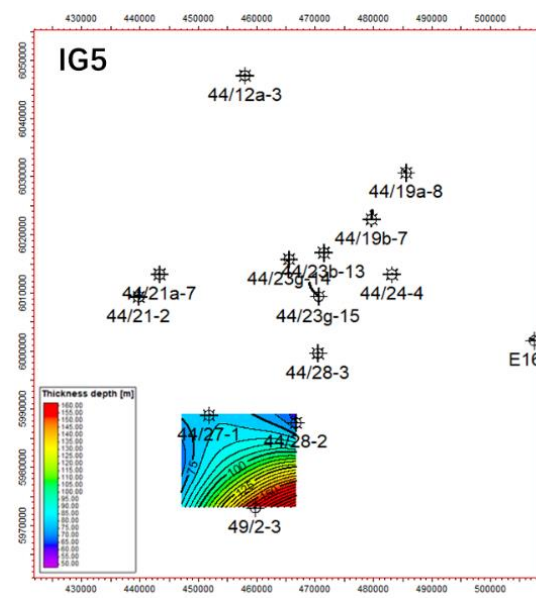
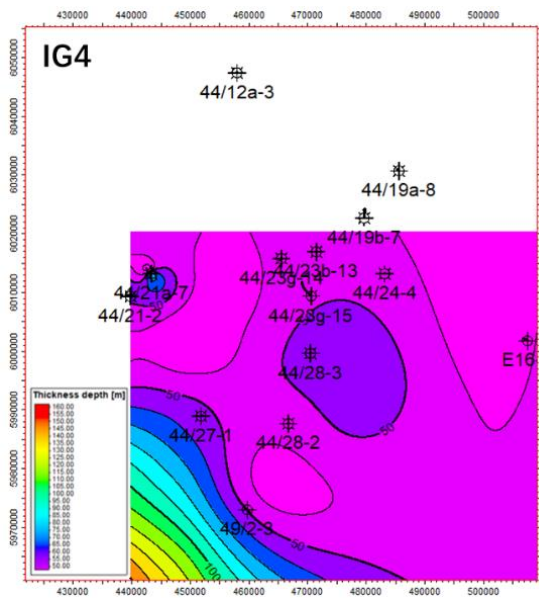
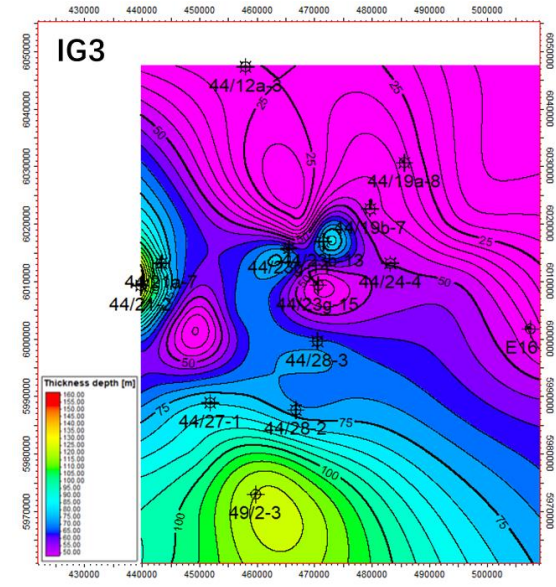
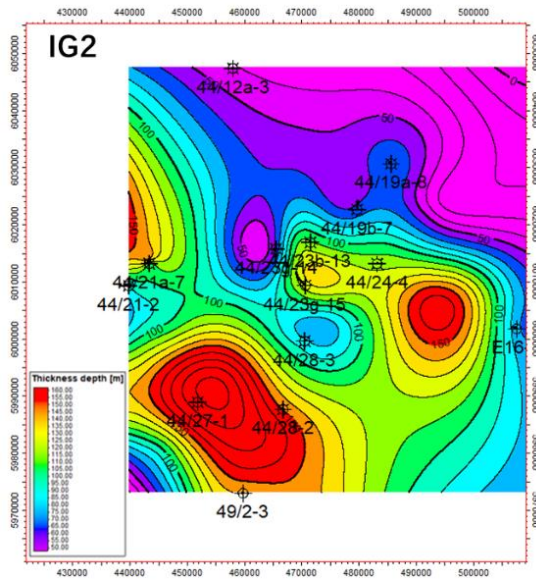
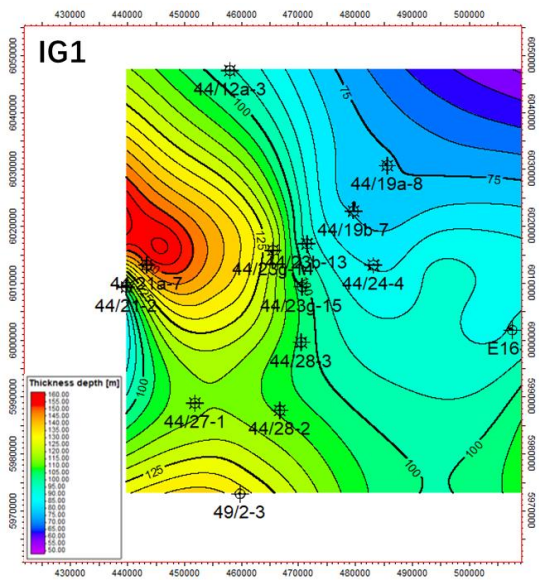


Panel A: The distribution of the thickness of each biozone in 16 wells. The thickness distribution of the Caister sandstone layer and the total thickness of all recognized biozones in the Cleaver formation and Westoe Coal formation were also plotted. Panel B: Thickness distribution of each stratigraphic package in wells comprising of the Westoe Coal formation and Cleaver formation. Note that this section is different from the section on biozones.

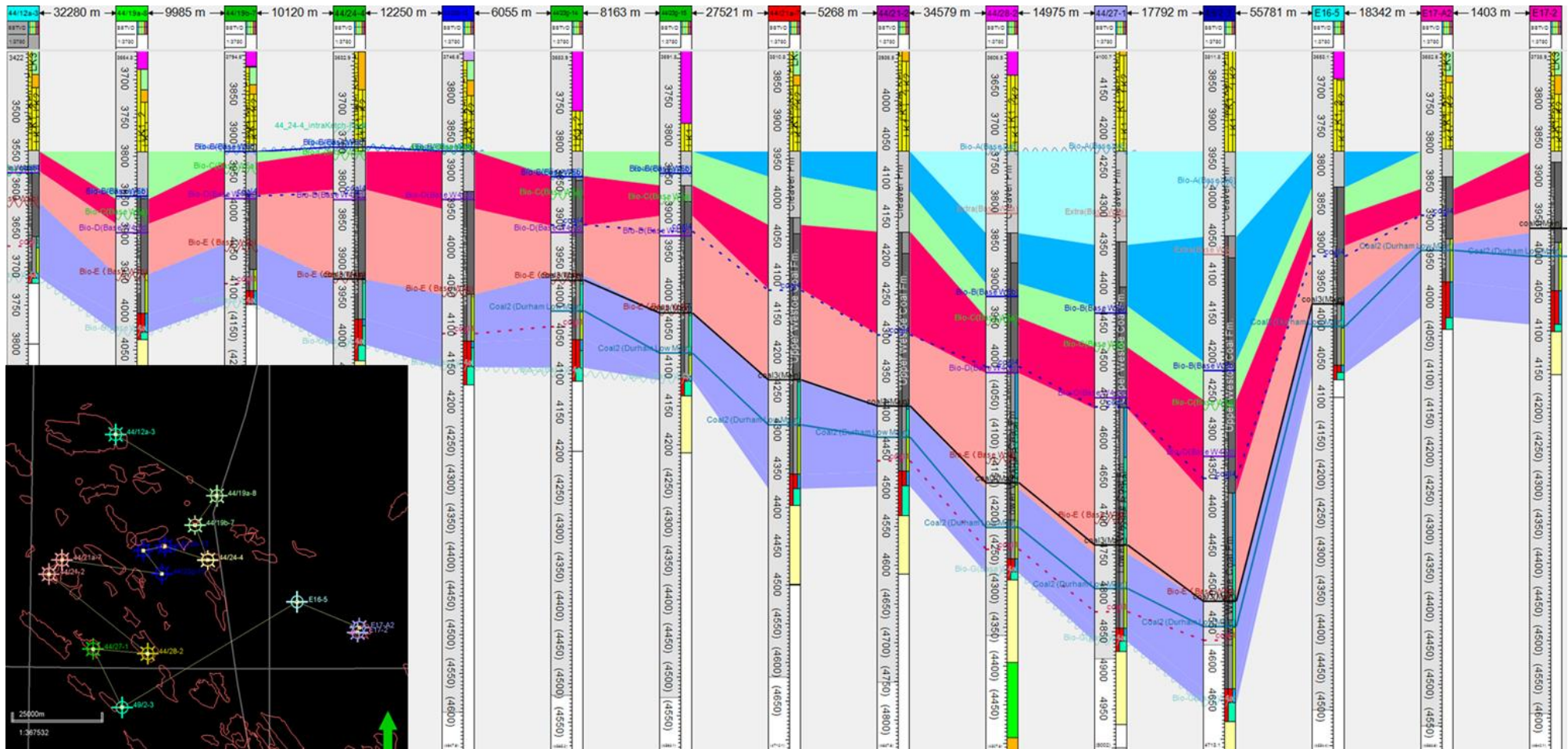
Appendix C. 2D map of each identified biozone.



Appendix D. 2D map of each INPEFA stratigraphic package.



Appendix E. Long section of integrated stratigraphy.



The background color represents the INPEFA stratigraphy. The biozones and coal seams correlation is marked by several lines.